Robust Optimal Energy Management of a Residential Microgrid Under Uncertainties on Demand and Renewable Power Generation

Postprint accepted for pubblication in *IEEE Transactions on Automation Science and Engineering*

How to cite: S. M. Hosseini, R. Carli and M. Dotoli, (2021) "Robust Optimal Energy Management of a Residential Microgrid Under Uncertainties on Demand and Renewable Power Generation," *IEEE Transactions on Automation Science and Engineering*, vol. 18, no. 2, pp. 618-637. DOI: 10.1109/TASE.2020.2986269

Robust Optimal Energy Management of a Residential Microgrid under Uncertainties on Demand and Renewable Power Generation

Seyed Mohsen Hosseini, *Student Member, IEEE*, Raffaele Carli, *Member, IEEE*, and Mariagrazia Dotoli, *Senior Member, IEEE*

***Abstract*— Smart microgrids are experiencing an increasing growth due to their economic, social and environmental benefits. However, the inherent intermittency of renewable energy sources (RESs) and users' behavior leads to significant uncertainty, which implies important challenges on the system design. Facing this issue, this paper proposes a novel robust framework for the day-ahead energy scheduling of a residential microgrid comprising interconnected smart users, each owning individual RESs, non-controllable loads (NCLs), energy-based and comfort-based controllable loads (CLs), and individual plug-in electric vehicles (PEVs). Moreover, users share a number of RESs and an energy storage system (ESS). We assume that the microgrid can buy/sell energy from/to the grid subject to quadratic/linear dynamic pricing functions. The objective of the scheduling is minimizing the expected energy cost while satisfying device/comfort/contractual constraints, including feasibility constraints on energy transferred between users and the grid under RES generation and users' demand uncertainties. To this aim, first, we formulate a min-max robust problem to obtain the optimal CLs scheduling and charging/discharging strategies of the ESS and PEVs. Then, based on the duality theory for multi-objective optimization, we transform the min-max problem into a mixed-integer quadratic programming problem to solve the equivalent robust counterpart of the scheduling problem effectively. We deal with the conservativeness of the proposed approach for different scenarios and quantify the effects of the budget of uncertainty on the cost saving, the peak-to-average ratio, and the constraints' violation rate. We validate the effectiveness of the method on a simulated case study and we compare the results with a related robust approach.**

***Note to practitioners*— This paper is motivated by the emerging need for intelligent demand-side management (DSM) approaches in smart microgrids in presence of both power generation and demand uncertainties. The proposed robust energy scheduling strategy allows the decision maker (i.e., the energy manager of the microgrid) to make a satisfactory trade-off between the users' payment and constraints' violation rate considering the energy cost saving, the system technical limitations and the users' comfort by adjusting the values of the budget of uncertainty. The proposed framework is generic and flexible as it can be applied to different structures of microgrids considering various types of uncertainties in energy generation or demand.**

***Index Terms*— Demand-side management, microgrid, optimal energy scheduling, mixed-integer quadratic programming, optimization, robust control.**

NOMENCLATURE

Acronyms

CL	Controllable load
DSM	Demand-side management
DWT	Domestic wind turbines
ECC	Energy consumption controller
EMS	Energy management system
ESS	Energy storage system
HP	Heat pump
HVAC	Heating, ventilation and air conditioning
H2V	Home to vehicle
LAN	Local area network
MILP	Mixed-integer linear programming
MIQP	Mixed-integer quadratic programming
NCL	Non-controllable load
PAR	Peak-to-average ratio
PEV	Plug-in electric vehicle
PoR	Price of robustness
PVS	Photovoltaic system
RES	Renewable energy source
V2H	Vehicle to home

Sets and Indices

$\mathcal{N}$	Set of users
$\mathcal{M}$	Set of RESs
$\mathcal{P}$	Set of uncertainty sources (RES/NCL)
$\mathcal{H}$	Time horizon
n	Index of users
m	Index of RESs
p	Index of uncertain sources
h	Index of time slots

Parameters

N	Number of users

Manuscript received on July 31, 2019; revised January 31, 2020, accepted on March 11, 2020 (*Corresponding author: Raffaele Carli*).

The work of M. Dotoli is partially supported by Italian University and Research Ministry under project RAFAEL (National Research Program, contract n. ARS01_00305).

The authors are with the Department of Electrical and Information Engineering of the Polytechnic of Bari, Bari 70125, Italy. E-mail addresses: {seyedmohsen.hosseini, raffaele.carli, mariagrazia.dotoli}@poliba.it.

M Number of RESs
P Number of uncertainty sources
H Number of slots in the time horizon
Δh Length of time slot
$\boldsymbol{r}_m$ Forecasted energy produced by mth RES
$\boldsymbol{b}_n$ Forecasted NCL demand of nth user.
$\overline{\boldsymbol{l}}_n/\underline{\boldsymbol{l}}_n$ Maximum/minimum CL energy level of nth user
L_n Total CL energy requirement of nth user.
τ_n Constant time of the first order dynamic of the nth user's household indoor temperature
π_n Total heating/cooling gain in the nth user's household
$\boldsymbol{T}^{ext}$ Forecasted outdoor temperature
$\boldsymbol{T}_n^{min}$, $\boldsymbol{T}_n^{max}$ Lower and upper bounding of the nth user's household Indoor temperature comfort range
E_n Maximum HP energy level for the nth user
k_n^s/k_n^f Plugged-in/out time slot of the PEV of nth user
v_n^0 Initial battery charge level of the PEV of nth user
V_n Final desired battery charge level of the PEV of nth user
$\overline{V}_n/\underline{V}_n$ Maximum/minimum battery capacity of the PEV of nth user
$\overline{v}_n/\underline{v}_n$ Maximum battery charging/discharging rates of the PEV of nth user.
ζ_n^+/ζ_n^- Charging/discharging battery efficiencies of the PEV of nth user
s^0 Initial charge level of the shared ESS
$\overline{s}/\underline{s}$ Maximum charging/discharging rates of the shared ESS
$\overline{S}/\underline{S}$ Maximum/minimum battery capacity of the shared ESS
η^+/η^- Charging/discharging battery efficiencies of the shared ESS
$\overline{g}/\underline{g}$ Maximum buyable/saleable energy from/to the power grid
$\boldsymbol{k}^+/\boldsymbol{k}^-$ Cost coefficients of buying/selling energy from/to the power grid
$\boldsymbol{d}_p$ Nominal profile for the pth source of uncertainty
$\tilde{\boldsymbol{d}}_p$ Uncertain profile for the pth source of uncertainty
$\hat{\boldsymbol{d}}_p$ Semi-amplitude profile of the maximum deviation for the pth source of uncertainty
Γ_0 Budget of uncertainty
w_0 Weight associated to the protection function of the objective function
w_h Weight associated to the protection function of the inequality constraints at the hth time slot

Continuous decision variables
$\boldsymbol{x}_n^l$ CL demand profile for the nth user
$\boldsymbol{x}_n^p$ HP demand profile for the nth user
$\boldsymbol{T}_n$ Household indoor temperature profile for the nth user
$\boldsymbol{x}_n^v$ PEV stored/released energy profile for the nth user
$\boldsymbol{x}_n^{v\delta}$ Supporting variables aimed at modelling the PEV of the nth user
$\boldsymbol{v}_n$ Battery charge level of the PEV of nth user.
$\boldsymbol{x}^s$ Stored/released energy profile for the shared ESS
$\boldsymbol{x}^{s\delta}$ Supporting variables aimed at modelling the shared ESS
$\boldsymbol{s}$ Battery charge level profile for the shared ESS
$\boldsymbol{x}^g$ Energy exchanged between the microgrid and the power grid
$\boldsymbol{x}^{g\delta}$ Supporting variables aimed at modelling the energy exchange between the microgrid and the power grid
$\boldsymbol{x}^a$ Supporting variable related to the energy scheduling formulation
Γ_h Portion of the budget of uncertainty Γ_0 allocated to the hth time slot
$\alpha, \boldsymbol{x}_p^b$ Supporting variable related to the robust counterpart formulation
$\boldsymbol{y}, \Lambda, \boldsymbol{\lambda}, \boldsymbol{\theta}_{ph}, \Theta_{ph}$ Supporting variables related to the robust counterpart reformulation
$\boldsymbol{u}_p$ Supporting variables representing the levels of variation of the pth source of uncertainty

Discrete decision variables
$\boldsymbol{\delta}_n^v$ Binary variables representing the charging or discharging mode of PEV for the nth user over the time horizon
$\boldsymbol{\delta}^s$ Binary variables representing the charging or discharging mode of the shared ESS over the time horizon
$\boldsymbol{\delta}^g$ Binary variables representing the mode of buying or selling energy from/to the power grid over the time horizon
$\mathcal{Q}_h$ Supporting variable representing the subset of indices related to the sources of uncertainty affected by the maximum deviation in the hth time slot
q_h Supporting variable representing the index of the source of uncertainty affected by a variation lower than the maximum deviation in the hth time slot

I. Introduction

THE application of intelligent demand-side management (DSM) to smart grids is rapidly gaining momentum in research and industry [1]-[3]. The ability of DSM in load curve shaping is of interest for the effective management of residential energy systems, which currently account for 30% of the total primary energy consumption of the world and 36% of the European Union's (EU) emission [4], [5]. Accordingly, residential load scheduling has attracted significant attention. Indeed, the components of a residential smart grid can cooperate through an energy management system (EMS) for optimal demand response of the end-users, and for efficient interaction of power grid, smart appliances, renewable energy sources (RESs), energy storage systems (ESSs) and plug-in electric vehicles (PEVs) [6]. However, an important challenge for residential energy scheduling is that the inherent intermittency of RES generation (e.g., photovoltaic systems (PVSs) or domestic wind turbines (DWTs)) imposes significant forecast uncertainty to the supply side [7]. On the other hand, the users' energy demand profile of small-scale residential microgrids is largely affected by demand-side uncertainty, due to the unpredictable changes in users' preferences. In this context, the presence of forecast noise may endanger the security of the system operation [8]. Moreover, uncertainty in forecast data can dramatically reduce economic and environmental benefits, customer comfort and may impose

system technical limitations. Hence, inaccuracies in forecast data impose many challenges to the design of an optimal energy scheduling [9], [10]. Therefore, the necessity of developing an effective optimal energy scheduling framework tackling the issue of forecast uncertainty is apparent [11]. Coping with this challenge, in this work we present a robust framework for day-ahead energy scheduling of a group of interconnected smart homes under RES generation and users' behavior uncertainties. From the controllability point of view, we divide home appliances into controllable loads (CLs), with flexible and programmable operation, and non-controllable loads (NCLs), with inflexible and fixed power curve [12], [13]. In our framework, we assume that each user incorporates NCLs, an energy-based CL, a comfort-based CL such as a heat pump (HP), an individually-owned RES, and a PEV with vehicle-to-home (V2H) and home-to-vehicle (H2V) operating modes [14]. Moreover, all users share an ESS, and a number of PVSs and DWTs as well. Our main objective is minimizing the total energy payment for the microgrid while satisfying the related constraints in presence of forecast uncertainty in RES generation and users' demand. We aim at obtaining a robust solution, including the optimal scheduling of the CLs for each user and the charging/discharging strategies of the shared ESS and individual PEVs at each time slot. Hence, we present a tractable robust optimization scheme to solve the energy scheduling problem with a quadratic cost function, which realistically models the cost of energy bought from the grid. Also, the microgrid is able to sell the energy back to the grid by a linear cost function. All the related device/comfort/contractual constraints, including specifically a contractual obligation imposed by the power grid restricting the users' exchanged energy over time slots, are modeled. First, a deterministic model of the scheduling problem is formulated. Hence, a min-max robust counterpart considering uncertain parameters is established regarding the cardinality-constrained uncertainty set. We finally apply some mathematical transformations to solve the equivalent problem effectively. We also investigate the effect of the proposed approach on the peak-to-average ratio (PAR) of the total exchanged energy. We deal with the robustness of the proposed approach against the level of conservativeness of the solution.

This paper is organized as follows. Section II provides an overview of the literature on microgrid energy scheduling in presence of uncertainty and positions the paper contribution. Section III describes the detailed model of the system under study. The deterministic and robust formulations of the scheduling problem are presented in Section IV and Section V, respectively. The case study results and analysis are provided in Section VI to demonstrate the benefits of the proposed strategy in comparison with a related robust approach. Finally, the paper ends with conclusions and future work in Section VII.

II. Related Work and Paper Contributions

In the field of DSM, several researchers have investigated the optimal energy scheduling of smart household appliances [12]-[34]. Generally, the scheduling seeks to provide optimal operational plans for electrical appliances in order to minimize the expected cost of performing all required tasks or to maximize the environmental benefits. The objective function is typically a dynamic (time-varying) function of the daily costs of the energy consumption subject to various technical, comfort, operational and energy balance constraints [14]. To provide energy in a reliable way, utility companies mainly use generators burning fossil fuels. Accordingly, in numerous research works the power generation cost is assumed to be a quadratic function of the energy consumption [15]-[21]. For instance, [16] and [17] propose incentive-based energy scheduling mechanisms for smart homes considering tractable quadratic cost functions. A distributed bi-level residential energy management is presented in [18] by formulating a multi-objective constrained non-linear problem to optimize electricity cost, discomfort, and appliance interruptions. In the context of energy scheduling under uncertainty, one of the widely used strategies for DSM is known as stochastic optimization based on statistical data [22]-[26]. In this context, for example, Kim *et al.* [22] present a stochastic dynamic programming for energy scheduling based on statistical knowledge about future prices to find decision thresholds for both noninterruptible and interruptible loads. In [23], a stochastic optimization framework for energy management of a smart home is proposed coping with the uncertainty associated with RES generation and PEV's plug-state as a Markov decision process. A probability distribution model combining household power consumption, PEV home-charging and RES generation is developed by Munkhammara *et al.* [24] through a convolution approach to merge three separate existing probability distribution models. In [26], an energy scheduling scheme for the optimal energy management of a microgrid utilizing the probabilistic forecasts of wind power and users' energy demand is presented. First, they formulate the energy scheduling problem as a stochastic model predictive control problem, and then convert it to a standard convex quadratic programming using machine-learning techniques.

Although stochastic DSM methods show effective performance facing uncertainty in resources availability or demand, they suffer from some serious limitations: for example, large presence of uncertain data which need to be modeled, dependency between some uncertain parameters, insufficient historical data for new houses, and high computational effort due to significant number of scenarios impose additional difficulty and cost to such models [14], [27]. Hence, dealing with the mentioned issues of stochastic-based approaches, robust optimization was proposed as an alternative promising solution [27]-[34]. A comparison between robust optimization and stochastic optimization approaches for energy scheduling of residential appliances under uncertainties in real-time electricity prices is provided in [27]. The authors prove that robust optimization has a significantly better computational performance. Moreover, modeling uncertainty through robust optimization using data intervals is simpler than modeling uncertainty by stochastic optimization, which requires random variables with detailed statistical information [27]. Among the research efforts towards energy scheduling utilizing robust optimization, [28] discusses the robust optimal scheduling of a

residential smart grid incorporating an ESS under uncertainty in energy price. The authors assume that the uncertain energy prices are randomly distributed with a known probability distribution around the predicted values. In [29], a robust optimization approach is proposed considering the uncertain output variation of RESs. A two-stage complementary framework is adopted to plan the collaborative scheduling of the ESS with an incentive-based demand response program called Direct Load Control (DLC) which directly shuts down the remote CLs to maintain the power balance in a microgrid. A multi-objective robust scheduling model is established in [30], where both supply and demand sides are affected by uncertainty. The aim is to obtain the lowest operating cost and the highest renewable energy utilization rate. The uncertain problem is transformed into a deterministic problem and a genetic algorithm is used to solve the deterministic problem. Wang *et al.* [31] develop a robust optimization approach with adjustable robustness level for household load scheduling considering power uncertainty of household photovoltaic system. The authors formulate the day-ahead load scheduling problem as a min-max uncertain problem considering interval-based uncertain parameters, and then transform it into the robust counterpart. However, they adopt a linear cost function for the energy exchanged with the grid, and they do not address the uncertainty associated with users' behavior. Paul and Padhy [32] adopt robust conditional value at risk optimization as a linear risk measure approach to protect the day-ahead residential energy scheduling against uncertainties associated with RES generation and energy price volatility. In [33], the robust optimal energy scheduling of a smart grid affected by uncertainty is investigated. The authors establish a mixed-integer linear programming (MILP) formulation to minimize the overall energy cost. However, the focus of this work is on the uncertainty associated with price signals, and on analyzing the effect of price uncertainty on the operation of the smart grid's components, which is different than our focus that is on uncertainty related to users' behavior and RES energy generation. In a related work, Paridari *et al.* [34] deal with the robust energy scheduling of smart home appliances comprising the ESS unit, taking the uncertain behavior of users into account. Although it deals with uncertainty in load demand, such a work focuses on uncertainty associated with CLs as decision variables, that is different than our focus on uncertainty involved with NCLs. The authors map the load uncertainty to the cost function coefficients and formulate the problem as a MILP. In addition, the uncertainty associated with RES energy generation is not considered in that work. Moreover, unlike our work, all the aforementioned studies [27] to [34] adopt a linear cost function for energy bought from the power grid, and do not take the effect of uncertainty in the feasibility of energy exchange between users and power grid into account. Additionally, the effects of the energy scheduling method on the PAR of the total energy demand are not quantified in the mentioned works.

Regarding other robust optimization methods addressing uncertainty in parameters, we can refer to two-stage robust methods, including affine adjustable robust counterpart approaches [35], [36]. There can be found different types of multi-stage robust optimization methods in the literature, mainly solved by two classes of algorithms, namely Benders and column-and-constraint generation algorithms. The former approach is based on applying decomposition techniques to transform the original two-stage problem into a single-stage problem, and then utilizing the Benders algorithm to solve the reformulated problem [35]. On the contrary, the latter approach is based on the column-and-constraint generation, which leads to critical uncertain scenarios, requiring recourse decision variables and second-stage constraints to solve the reformulated problem [36].

However, as our energy scheduling problem has a quadratic objective function with several binary variables, applying these two-stage robust approaches, where the optimization problem is set as a min-max-min problem which is needed to be dualized by adding extra bilinear terms in the objective function, can result in an extremely large-scale mixed-integer quadratic programming (MIQP) model, which is more computationally expensive and more complicated than our proposed single-stage robust technique. Therefore, the scheduling is most likely to be intractable with the increase of the problem size for large-scale microgrid where the number of components (in particular, energy storage systems or plug-in electric vehicles) in the microgrid increases [35], [37]. Another robust method to address uncertainty in optimization problems is based on the affine adjustable robust counterpart assuming affine functions of uncertain parameters for resource decisions [38], [39]. However, in contrast with our case, such a class of robust approaches is generally unable to handle problems with integer resource decisions [35], [37], [40]. Moreover, this method typically needs full knowledge about the past data on the uncertain demand to derive a decision by inserting them in a linear decision rule, which is mostly unavailable [41]. The advantage of our robust optimization framework is that it is more general and applicable to a wide spectrum of demand-side management problems. In addition, the final problem is tractable and can be easily implemented by using commercial optimization tools. We better highlight these advantages of our method in the case study section.

Hence, although some studies have made positive attempts for optimizing the energy scheduling of residential microgrids in presence of forecast uncertainties, due to their respective limitations, further research is still required to cope with the challenge of RES energy generation and users' behavior uncertainty in residential load scheduling. Summing up, the specific contributions of this work lie in the following aspects.

1) We present a comprehensive model and a systematic robust methodology to state and solve the optimal energy scheduling problem of a grid-connected residential microgrid with several users incorporating individually owned RESs, NCLs, energy-based and comfort-based CLs, and PEVs. Moreover, the smart users share a given number of RESs and an ESS under a dynamic quadratic pricing. However, the microgrid is also able to sell its extra energy back to the grid by a dynamic linear pricing. We take the forecast uncertainty caused by the RESs energy profiles, as well as the users' energy

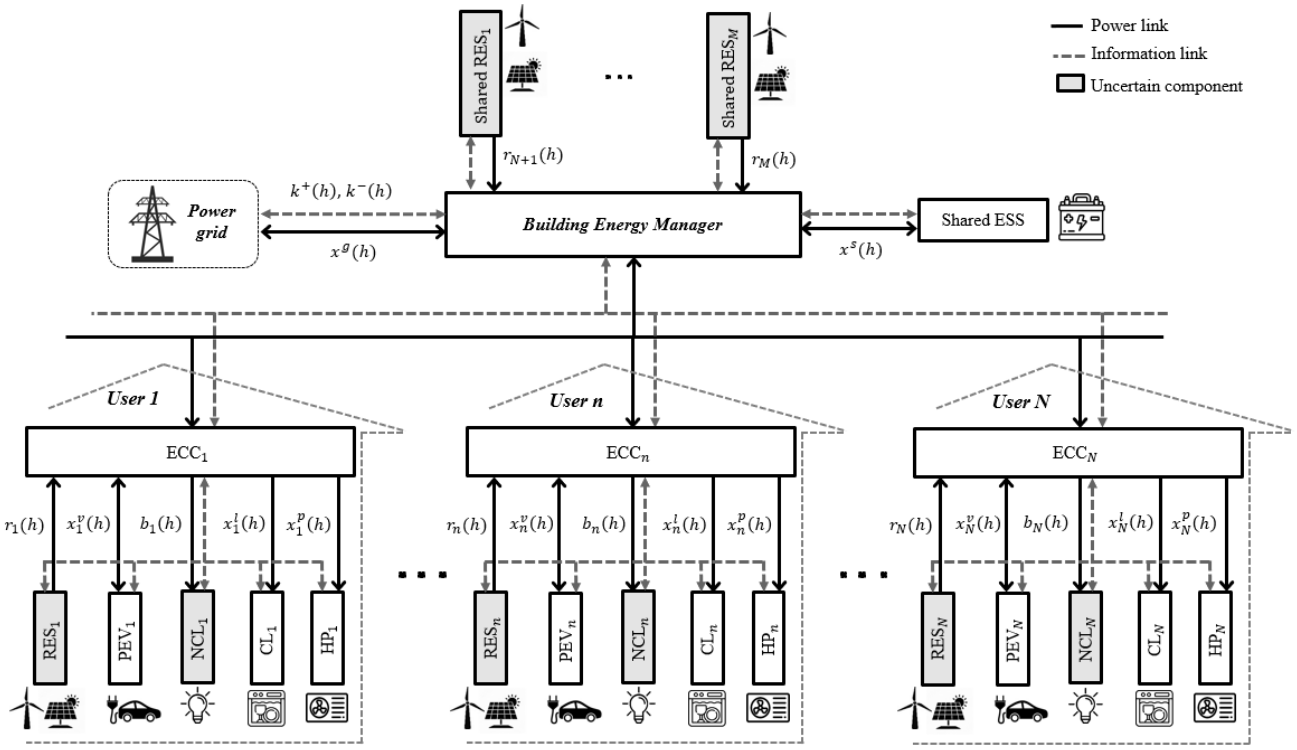

Fig. 1. Scheme of energy flows and connections between distribution network, users' energy system components, and shared devices.

demand, into account.

2) We establish a quadratic min-max robust problem under the cardinality-constrained uncertainty set inspired by the method proposed by Bertsimas and Sim [42], and convert it to a MIQP model to solve the equivalent robust counterpart of the scheduling problem. Forecast uncertainty in both the objective function and corresponding contractual constraints is addressed. The problem includes uncertain terms both in the objective function and in the left-hand side (LHS) and the right-hand side (RHS) of the inequality constraints. To the best of the authors' knowledge, no robust quadratic programming approach for the energy scheduling of the residential microgrid has ever been proposed to tackle the uncertainties associated with RES energy generation and users' energy demand under quadratic pricing.

3) Our proposed framework is generic and flexible as it can be applied to different structures of microgrids considering various types of uncertainties in energy generation or demand.

4) We deal with the conservativeness of the proposed scheme for different scenarios and quantify the effects of the budget of uncertainty on the cost saving, the PAR and constraints' violation rate. Our robust approach enables the decision maker (i.e., the energy manager of the microgrid) to make a trade-off between the users' payment and constraints' violation rate by adjusting the values of the budget of uncertainty.

We validate the effectiveness of the proposed approach on a sample residential microgrid with several users under forecast uncertainty. We also provide a comprehensive comparison between our proposed robust energy scheduling and energy scheduling with an exact forecast profile without protection against data uncertainty. To better show the advancement of our approach with respect to the related literature, we also compare the results of our proposed approach with a related robust method, confirming the performance of the proposed framework.

III. System Model

In this section, we present a mathematical model of the day-ahead energy scheduling problem for the users' appliances and PEVs, the individual and shared resources (i.e., the RESs and the ESS), as well as the demand-supply balance and constraints.

The features of the considered microgrid are defined according to residential microgrid architectures commonly used in the most recent studies. For instance, based on the well-known definitions and system structures provided in [43]-[46], a residential microgrid can be considered as a locally controlled system to promote the integration of distributed generation sources, energy storage systems, interconnected users with household loads, plug-in electric vehicles along with smart meters and home energy consumption controllers, in which households' energy demands can be supplied by local generations while their extra required/surplus energy can be bought/sold from/to the power grid. The architecture of the considered system is shown in Fig. 1. We assume that each user owns a smart meter comprising an energy consumption controller (ECC). The ECC is in charge of controlling the user's energy consumption and enforcing the collaboration in the microgrid. The activities of all the smart users are controlled by the energy management system (EMS) that is also in charge of acquiring pricing signals from the power grid and managing the operations of shared resources. A digital communication infrastructure (e.g., a local area network (LAN)) is implemented

to connect all the microgrid components to the energy management system [43]. For the ease of implementation, we assume that each user comprises one RES, one NCL, one CL, one Heat Pump (HP), and one PEV only, but the model can be straightforwardly expanded to scenarios with several loads and PEVs for each user. Let $\mathcal{N} \triangleq \{1, \dots, n, \dots, N\}$ denotes the set of users. We consider a time window $\mathcal{H} \triangleq \{1, \dots, h, \dots, H\}$ including H discrete time slots with equal length Δh. In the following, vectors are denoted by bold letters. The microgrid model is detailed in the sequel.

A. Renewable Energy Sources

We assume that the microgrid incorporates a number M of RESs, (e.g., photovoltaic systems or domestic wind turbines) denoted as $\mathcal{M} \triangleq \{1, \dots, m, \dots, M\}$ including both the RESs that are shared and those that are individually owned by users ($M > N$). We define M column vectors of H input parameters $\boldsymbol{r}_m \triangleq [r_m(1); \dots; r_m(h); \dots; r_m(H)]$ $(m \in \mathcal{M})$ collecting the energy profiles produced by the RESs. These vectors are assumed to be calculated by a forecast sub-module of the EMS using a prediction algorithm based on weather data [47].

B. Users' Energy Loads

First of all, we assume that users are equipped with NCLs, which are inflexible loads, whose operation time cannot be shifted and whose profile cannot be modulated (i.e., with fixed power profile). We introduce N column vectors of H input parameters $\boldsymbol{b}_n \triangleq [b_n(1); \dots; b_n(h); \dots; b_n(H)]$ $(n \in \mathcal{N})$ to denote the users' NCL profiles. We assume that these vectors are computed by forecast sub-modules of the ECCs using a prediction algorithm [48]. We show in Section V.B that, in order to solve the scheduling problem, our approach only requires knowledge of the lower and upper bounds of the NCLs profiles as well as RESs production curves, which are typically available based on historical data.

Second, we assume that users are also equipped with CLs, which are loads with flexible and programmable operations. Such controllable loads can be operated on a favorable schedule. CLs can be commonly categorized into two different classes [49]: 1) energy-based CLs: these appliances are characterized by a prescribed energy requirement (e.g., pumps of waters supply networks, EVs), i.e., a certain amount of energy has to be consumed over a set of time slots delimited by a minimum starting-time slot and a maximum ending-time slot; 2) comfort-based CLs: these devices consume energy to control a physical variable influencing the user's comfort (e.g., heating, ventilation and air conditioning (HVAC) systems, refrigerators). Without loss of generality, we assume that for each user one CL for each class is identified.

As for the energy-based CLs, we introduce a column vector $\boldsymbol{x}_n^l \triangleq [x_n^l(1); \dots, x_n^l(h); \dots, x_n^l(H)]$ for each user $n \in \mathcal{N}$ with H decision variables referring to the consumption profile of the CL. We collect all the users' CL profiles in a column vector $\boldsymbol{x}^l \triangleq [\boldsymbol{x}_1^l; \dots; \boldsymbol{x}_N^l]$ whose length is NH. Due to operational requirements, users' loads are restricted by minimum and maximum operating levels. We use two column vectors of H input parameters $\overline{\boldsymbol{l}}_n \triangleq \left[\overline{l}_n(1); \dots, \overline{l}_n(h); \dots, \overline{l}_n(H)\right]$ and $\underline{\boldsymbol{l}}_n \triangleq \left[\underline{l}_n(1); \dots; \underline{l}_n(h); \dots; \underline{l}_n(H)\right]$ to indicate the maximum and minimum energy level for each user n, respectively. Furthermore, a constraint should be enforced for each user to make sure that the cumulative energy fulfills the total energy requirement, denoted as L_n $(n \in \mathcal{N})$, by the deadline to complete the task at the end of the time window:

$$\underline{\boldsymbol{l}}_n \leq \boldsymbol{x}_n^l \leq \overline{\boldsymbol{l}}_n,\ n \in \mathcal{N} \tag{1}$$

$$\sum_{h=1}^{H} x_n^l(h) = L_n, \quad n \in \mathcal{N}. \tag{2}$$

As for the comfort-based CLs, just to fix ideas, we refer to the HVAC heat pumps (HPs) serving the users' household indoor environment. The following discrete time model can be used to represent the nth user's indoor temperature [50]:

$$\begin{aligned} T_n(h) &= e^{-\Delta h/\tau_n}\, T_n(h-1) \\ &+(1-e^{-\Delta h/\tau_n})(T^{ext}(h) + \pi_n x_n^p(h)), h \in \mathcal{H}, n \in \mathcal{N} \end{aligned} \tag{3}$$

where $T_n(h)$ and $T_{ext}(h)$ are the household indoor and outdoor temperatures at time slot h, respectively, τ_n is the time constant of the first order dynamics of the household indoor temperature, π_n is the total heating/cooling gain in the considered environment ($\pi_n > 0$ if the HVAC system is in heating mode and $\pi_n < 0$ if the HVAC system is in cooling mode), and $x_n^p(h)$ is the heat pump consumption at time slot h. Note that vector $\boldsymbol{T}^{ext}(t) \triangleq [T^{ext}(1); \dots; T^{ext}(h); \dots; T^{ext}(H)]$ collecting the outdoor temperature profiles in the time window $\mathcal{H}$ is an input parameter, computed using weather prediction data. Conversely, vector $\boldsymbol{T}_n \triangleq [T_n(1); \dots; T_n(h); \dots; T_n(H)]$ collecting for each user $n \in \mathcal{N}$ the household indoor temperature profile is a variable of the problem. Vector $\boldsymbol{T}_n$ has to be computed in accordance with the following constraint:

$$T_n^{min}(h) \leq T_n(h) \leq T_n^{max}(h), \quad h \in \mathcal{H}, n \in \mathcal{N} \tag{4}$$

where $\boldsymbol{T}_n^{min} \triangleq [T_n^{min}(1); \dots; T_n^{min}(h); \dots; T_n^{min}(H)]$ and $\boldsymbol{T}_n^{max} \triangleq [T_n^{max}(1); \dots; T_n^{max}(h); \dots; T_n^{max}(H)]$ denote the vectors of lower and upper bounding of the nth user's household indoor temperature, respectively. Range $[T_n^{min}(h), T_n^{max}(h)]$ $(h \in \mathcal{H})$ is a time-varying parameter that allows users to represent thermal comfort preferences within the occupancy period. Similarly, vector $\boldsymbol{x}_n^p \triangleq [x_n^p(1); \dots; x_n^p(h); \dots; x_n^p(H)]$ collecting for each user $n \in \mathcal{N}$ the heat pump consumption profile is a variable of the problem. Vector $\boldsymbol{x}_n^p$ has to be computed in accordance with the following constraint:

$$0 \leq x_n^p(h) \leq E_n, \quad h \in \mathcal{H}, n \in \mathcal{N} \tag{5}$$

where E_n is the maximum energy that the pump can consume in one time slot with duration Δh.

Third, we assume that users are also equipped with PEVs, which act as versatile active elements that are able to consume, store, and supply energy [51]. This means that the PEVs' battery charging is bidirectional, in accordance with the following modes of operation: H2V (home to vehicle, i.e., the charging of the PEV is a function of the total demand in the home, aiming at preventing overloads) and V2H (vehicle to home, i.e., the PEV is used to operate as an offline uninterruptible power supply) [51]. To model the charging/discharging activities of the PEV of user n within the time windows, we define a column vector $\boldsymbol{x}_n^v \triangleq$

$[x_n^v(1); \dots; x_n^v(h); \dots; x_n^v(H)]$, with H decision variables, where $x_n^v(h)$ is the energy stored/released in/by the PEV of user n at time slot h. Due to the conversion losses of the PEV, we define ζ_n^+ and ζ_n^- as the charging and discharging efficiencies for the PEV of user n, respectively.

Since PEVs may not be connected to the grid throughout the whole time window for various reasons (e.g., driving on the road), we assume that the PEV of each user $n \in \mathcal{N}$ is connected to the power system within a given plugged-in interval $[k_n^s, k_n^f]$. This interval is defined by users at the beginning of the scheduling horizon, e.g. on a daily basis, according to their preferences and PEVs' availability. During this interval, the PEV is plugged to the microgrid, and thus can be either charged or discharged:

$$x_n^v(h) = 0, h \in \mathcal{H} \backslash [k_n^s, k_n^f], n \in \mathcal{N} \tag{6}$$

$$\underline{v}_n \le x_n^v(h) \le \overline{v}_n \,, h \in [k_n^s, k_n^f], n \in \mathcal{N} \tag{7}$$

where we denote as $\overline{v}_n$ and $\underline{v}_n$ the maximum charging and discharging rates, respectively.

To avoid simultaneous charging and discharging of the PEV battery, the dynamics of the charge level of the PEV of user n can be written as a first order discrete time model as follows [10]:

$$v_n(h) = \begin{cases} v_n(h-1) + \zeta_n^+ x_n^v(h) \text{ if } x_n^v(h) \ge 0 \\ v_n(h-1) + x_n^v(h)/\zeta_n^- \text{ if } x_n^v(h) < 0 \end{cases}, \quad h \in [k_n^s, k_n^f], n \in \mathcal{N} \tag{8}$$

where $v_n(h)$ and $v_n(k_n^s - 1) \triangleq v_n^0$ denote the charge level of the PEV of user n at time slot h and the initial battery charge level at the beginning of plugged-in interval, respectively. In this work, we assume that the battery degradation and leakage effects are negligible. Moreover, we assume that the charge level of the PEV of user n at the end of plugged-in interval (i.e., $v_n(k_n^f)$) has to be equal to a given desired level V_n:

$$V_n = v_n(k_n^f). \tag{9}$$

The charge level is bounded by the minimum and maximum battery capacity $\underline{V}_n$ and $\overline{V}_n$ as follows:

$$\underline{V}_n \le v_n(h) \le \overline{V}_n \,, h \in [k_n^s, k_n^f], n \in \mathcal{N}. \tag{10}$$

Following [52], through the use of logical and supporting variables, we now transform (8) into a linear form. First, we introduce a column vector of H logical variables $\boldsymbol{\delta}_n^v \triangleq [\delta_n^v(1); \dots; \delta_n^v(h); \dots; \delta_n^v(H)]$, where each component $\delta_n^v(h)$ takes value 0 or 1 if the PEV stores (i.e., $x_n^v(h) \ge 0$) or releases (i.e.,$x_n^v(h) < 0$) energy, respectively:

$$\delta_n^v(h) \in \{0,1\}, h \in \mathcal{H}, n \in \mathcal{N} \tag{11}$$

$$\boldsymbol{x}_n^v \ge \mathbf{0}_{H,1} \Leftrightarrow \boldsymbol{\delta}_n^v = \mathbf{0}_{H,1}, n \in \mathcal{N} \tag{12}$$

where we denote as $\mathbf{0}_{n,1}$ the n-dimensional column vector with all elements equal to zero. Second, we introduce a supporting vector $\boldsymbol{x}_n^{v\delta} \triangleq [x_n^{v\delta}(1); \dots; x_n^{v\delta}(h); \dots; x_n^{v\delta}(H)]$ defined as follows:

$$\boldsymbol{x}_n^{v\delta} = \boldsymbol{\delta}_n^v \circ \boldsymbol{x}_n^v, n \in \mathcal{N} \tag{13}$$

where the symbol $\circ$ denotes the entrywise product. Note that logical equations (12)-(13) can be replaced with [54]:

$$\boldsymbol{x}_n^v \le \overline{v}_n(\mathbf{1}_{H,1} - \boldsymbol{\delta}_n^v), n \in \mathcal{N} \tag{14}$$

$$\boldsymbol{x}_n^v \ge \underline{v}_n \boldsymbol{\delta}_n^v, n \in \mathcal{N} \tag{15}$$

$$\boldsymbol{x}_n^{v\delta} \le \boldsymbol{x}_n^v - \underline{v}_n(\mathbf{1}_{H,1} - \boldsymbol{\delta}_n^v), n \in \mathcal{N} \tag{16}$$

$$\boldsymbol{x}_n^{v\delta} \ge \boldsymbol{x}_n^v - \overline{v}_n(\mathbf{1}_{H,1} - \boldsymbol{\delta}_n^v), n \in \mathcal{N} \tag{17}$$

$$\boldsymbol{x}_n^{v\delta} \le \overline{v}_n \boldsymbol{\delta}_n^v, n \in \mathcal{N} \tag{18}$$

$$\boldsymbol{x}_n^{v\delta} \ge \underline{v}_n \boldsymbol{\delta}_n^v, n \in \mathcal{N} \tag{19}$$

where we denote as $\mathbf{1}_{n,1}$ the n-dimensional column vector with all elements equal to one.

Using the above defined supporting vectors $\boldsymbol{\delta}_n^v$ and $\boldsymbol{x}_n^v$, (8) is thus transformed into a linear form:

$$v_n(h) = v_n(h-1) + \zeta_n^+(x_n^v(h) - x_n^{v\delta}(h)) + x_n^{v\delta}(h)/\zeta_n^-, \quad h \in [k_n^s, k_n^f], n \in \mathcal{N}. \tag{20}$$

Finally, we collect all the users' PEV decision variables vectors in column vectors $\boldsymbol{x}^v \triangleq [\boldsymbol{x}_1^v; \dots; \boldsymbol{x}_N^v]$, $\boldsymbol{x}^{v\delta} \triangleq [\boldsymbol{x}_1^{v\delta}; \dots; \boldsymbol{x}_N^{v\delta}]$, and $\boldsymbol{\delta}^{\mathrm{v}} \triangleq [\boldsymbol{\delta}_1^{\mathrm{v}}; \dots; \boldsymbol{\delta}_{\mathrm{N}}^{\mathrm{v}}]$, whose lengths are NH.

C. Shared Energy Storage System

The shared ESS unit provides flexibility to users in the scheduling energy consumption. Household energy storage devices are mainly batteries such as lead-acid and Li-ion [31]. Here the shared ESS is modeled as in [52]. The shared ESS should optimally store energy from the grid ahead of time and consume it during peak hours when the grid load demand is high. To model the charging/discharging activities of the ESS within the time windows, we define a column vector $\boldsymbol{x}^s \triangleq [x^s(1); \dots; x^s(h); \dots; x^s(H)]$, with H decision variables, where $x^s(h)/x^s(h)$ is the energy stored/released in/by the battery at time slot h. Due to the conversion losses of the ESS, we define η^+ and η^- as the charging and discharging efficiencies, respectively.

Similarly to the PEVs' model, the dynamics of the charge level of the ESS for $h \in \mathcal{H}$ can be written as a first order discrete time model as follows [12]:

$$s(h) = \begin{cases} s(h-1) + \eta^+ x^s(h) \text{ if } x^s(h) \ge 0 \\ s(h-1) + x^s(h)/\eta^- \text{ if } x^s(h) < 0 \end{cases}, h \in \mathcal{H} \tag{21}$$

where $s(h)$ and $s(0) \triangleq s^0$ denote the charge level of the ESS at time slot h and at the beginning of time horizon, respectively. In this work, we assume that the battery degradation and leakage effects are negligible. Moreover, we assume that the charge level at the last time slot $s(H)$ and at the beginning of the time window s^0 are equal since the final energy level is also the initial condition for the next time window of the scheduling:

$$s^0 = s(H). \tag{22}$$

The maximum charge level is bounded by the minimum and maximum battery capacity $\underline{S}$ and $\overline{S}$ as follows:

$$\underline{S} \leq s(h) \leq \overline{S}, h \in \mathcal{H}. \quad (23)$$

Similarly to the PEVs' model, through the use of logical and supporting variables, we now transform (21) into a linear form. First, we introduce a column vector of H logical variables $\boldsymbol{\delta}^s \triangleq [\delta^s(1); \dots; \delta^s(h); \dots; \delta^s(H)]$, where each component $\delta^s(h)$ takes value 0 or 1 if the ESS stores (i.e., $x^s(h) \geq 0$) or releases (i.e.,$x^s(h) < 0$) energy, respectively:

$$\delta^s(h) \in \{0,1\}, h \in \mathcal{H} \quad (24)$$

$$\boldsymbol{x}^s \geq \mathbf{0}_{H,1} \Leftrightarrow \boldsymbol{\delta}^s = \mathbf{0}_{H,1} \quad (25)$$

Second, we introduce a supporting vector $\boldsymbol{x}^{s\delta} \triangleq \left[x^{s\delta}(1); \dots; x^{s\delta}(h); \dots; x^{s\delta}(H)\right]$ defined as follows:

$$\boldsymbol{x}^{s\delta} = \boldsymbol{\delta}^s \circ \boldsymbol{x}^s, n \in \mathcal{N}. \quad (26)$$

Note that logical equations (25)-(26) can be replaced with [54]:

$$\boldsymbol{x}^s \leq \overline{s}(\mathbf{1}_{H,1} - \boldsymbol{\delta}^s) \quad (27)$$

$$\boldsymbol{x}^s \geq \underline{s}\boldsymbol{\delta}^s \quad (28)$$

$$\boldsymbol{x}^{s\delta} \leq \boldsymbol{x}^s - \underline{s}(\mathbf{1}_{H,1} - \boldsymbol{\delta}^s) \quad (29)$$

$$\boldsymbol{x}^{s\delta} \geq \boldsymbol{x}^s - \overline{s}(\mathbf{1}_{H,1} - \boldsymbol{\delta}^s) \quad (30)$$

$$\boldsymbol{x}^{s\delta} \leq \overline{s}\boldsymbol{\delta}^s \quad (31)$$

$$\boldsymbol{x}^{s\delta} \geq \underline{s}\boldsymbol{\delta}^s \quad (32)$$

where $\overline{s}$ and $\underline{s}$ are the maximum charging and discharging rates.

Using the above defined supporting vectors $\boldsymbol{\delta}^s$ and $\boldsymbol{x}^{s\delta}$, (21) is thus transformed into a linear form:

$$s(h) = s(h-1) + \eta^+(x^s(h) - x^{s\delta}(h)) + x^{s\delta}(h)/\eta^-, \quad h \in \mathcal{H}. \quad (33)$$

D. Demand-Supply Balance

To satisfy the power balance in the system, a demand-supply balance constraint should be fulfilled at each time slot h. We introduce $\boldsymbol{x}^g \triangleq [x^g(1), \dots, x^g(h), \dots, x^g(H)]$ as a column vector of H decision variables modeling the energy profile exchanged between users and the power grid within the time window. The following balance equation must be thus satisfied:

$$\sum_{n=1}^{N}(\boldsymbol{x}_n^l + \boldsymbol{x}_n^v + \boldsymbol{x}_n^p + \boldsymbol{b}_n - \boldsymbol{r}_n) + \boldsymbol{x}^s - \sum_{m=N+1}^{M}\boldsymbol{r}_m = \boldsymbol{x}^g. \quad (34)$$

Finally, for the sake of keeping notations lightened, we rename the $P \triangleq N + M$ vectors of optimization input parameters with $\boldsymbol{d}_p \in \mathbb{R}^H$ ($p \in \mathcal{P} \triangleq \{1, \dots, P\}$), as follows:

$$\boldsymbol{d}_p = \begin{cases} \boldsymbol{b}_p \text{ if } p \in [1, N] \\ -\boldsymbol{r}_{p-N} \text{ if } p \in [N+1, N+M] \end{cases}, p \in \mathcal{P}. \quad (35)$$

In addition, we introduce a column vector $\boldsymbol{x}^a \triangleq [x^a(1); \dots; x^a(h); \dots; x^a(H)]$ of H supporting variables:

$$\boldsymbol{x}^a = \sum_{n=1}^{N}(\boldsymbol{x}_n^l + \boldsymbol{x}_n^v + \boldsymbol{x}_n^p) + \boldsymbol{x}^s \quad (36)$$

Hence, the energy balance equation (34) can be compactly rewritten as follows:

$$\boldsymbol{x}^a + \sum_{p=1}^{P}\boldsymbol{d}_p = \boldsymbol{x}^g. \quad (37)$$

E. Power Grid Energy Pricing and Constraints

A contractual obligation is enforced by the energy provider as an additional constraint, restricting the residual microgrid energy that could be bought/sold from/to the power grid to a maximum level at each time slot. We denote the maximum purchasable and salable energy profile imposed by the energy provider as a column vector $\overline{\boldsymbol{g}} \triangleq [\overline{g}(1); \dots; \overline{g}(h); \dots; \overline{g}(H)]$ and $\underline{\boldsymbol{g}} \triangleq \left[\underline{g}(1); \dots; \underline{g}(h); \dots; \underline{g}(H)\right]$, respectively. Thus, the values of the exchanged energy per time slot $x^g(h)$ ($h \in \mathcal{H}$) must be subject to the following constraints:

$$\underline{g}(h) \leq x^g(h) \leq \overline{g}(h), h \in \mathcal{H}. \quad (38)$$

Furthermore, we assume that the residential microgrid cannot simultaneously buy and sell energy from an imbalance in the energy prices of energy bought/sold from/to the power grid. We consider two different sets of pricing functions for the energy bought/sold from/to the grid. In particular, we assume that the pricing function for the energy bought from the main grid is a quadratic function like in [15]-[21]. On the other hand, we assume that the pricing function for the energy sold to the main grid is linear [32], [53]. Consequently, the cost function incurred by the microgrid at the hth time slot is defined as follows:

$$C_h(x^g(h)) = \begin{cases} k^+(h)(x^g(h))^2 \text{ if } x^g(h) \geq 0 \\ k^-(h)x^g(h) \text{ if } x^g(h) < 0 \end{cases}, h \in \mathcal{H} \quad (39)$$

where $\boldsymbol{k}^+ \triangleq [k^+(1); \dots; k^+(h); \dots; k^+(H)]$ and $\boldsymbol{k}^- \triangleq [k^-(1); \dots; k^-(h); \dots; k^-(H)]$ are column vectors collecting the known time-varying cost coefficients of buying/selling energy from/to the power grid, respectively.

Through the use of logical and supporting variables, we now transform (39) into a quadratic form. First, we introduce a column vector of H logical variables $\boldsymbol{\delta}^g \triangleq [\delta^g(1); \dots; \delta^g(h); \dots; \delta^g(H)]$, where each component $\delta^g(h)$ takes value 0 or 1 if the microgrid has an amount of energy to buy (i.e., $x^g(h) \geq 0$) or to sell (i.e., $x^g(h) < 0$), respectively:

$$\delta^g(h) \in \{0,1\}, h \in \mathcal{H} \quad (40)$$

$$\boldsymbol{x}^g \geq \mathbf{0}_{H,1} \Leftrightarrow \boldsymbol{\delta}^g = \mathbf{0}_{H,1}. \quad (41)$$

Second, we introduce a supporting vector $\boldsymbol{x}^{g\delta} \triangleq \left[x^{g\delta}(1); \dots; x^{g\delta}(h); \dots; x^{g\delta}(H)\right]$ defined as follows:

$$\boldsymbol{x}^{g\delta} = \boldsymbol{\delta}^g \circ \boldsymbol{x}^g. \quad (42)$$

Note that, following [54], logical equations (41)-(42) can be replaced with:

$$\boldsymbol{x}^g \leq \overline{\boldsymbol{g}} \circ (\mathbf{1}_{H,1} - \boldsymbol{\delta}^g) \quad (43)$$

$$\boldsymbol{x}^g \geq \underline{\boldsymbol{g}} \circ \boldsymbol{\delta}^g \quad (44)$$

$$\boldsymbol{x}^{g\delta} \leq \boldsymbol{x}^g - \underline{\boldsymbol{g}} \circ (\mathbf{1}_{H,1} - \boldsymbol{\delta}^g) \quad (45)$$

$$\boldsymbol{x}^{g\delta} \geq \boldsymbol{x}^g - \overline{\boldsymbol{g}} \circ (\mathbf{1}_{H,1} - \boldsymbol{\delta}^g) \quad (46)$$

$$\boldsymbol{x}^{g\delta} \le \overline{\boldsymbol{g}} \circ \boldsymbol{\delta}^{g} \tag{47}$$

$$\boldsymbol{x}^{g\delta} \ge \underline{\boldsymbol{g}} \circ \boldsymbol{\delta}^{g}. \tag{48}$$

Furthermore, using the above defined supporting vector $\boldsymbol{x}^{g\delta}$, the non-linear formulation of the energy cost at the hth time slot in (39) is thus transformed into a quadratic form:

$$\begin{aligned} C_h\left(x^{g}(h), x^{g\delta}(h)\right) = k^{+}(h)\left(x^{g}(h)\right)^2 \\ -k^{+}(h)\left(x^{g\delta}(h)\right)^2 + k^{-}(h)x^{g\delta}(h),\ h \in \mathcal{H}. \end{aligned} \tag{49}$$

The cost incurred by the residential microgrid to exchange the energy profile $\boldsymbol{x}^{g}$ with the power grid over the whole time window is the summation of costs over all the time slots, which is compactly written based on (49) as:

$$\begin{aligned} C\left(\boldsymbol{x}^{g}, \boldsymbol{x}^{g\delta}\right) = \sum_{h=1}^{H} C_h\left(x^{g}(h), x^{g\delta}(h)\right) = \\ \left(\boldsymbol{x}^{g}\right)^T \boldsymbol{K}^{+} \boldsymbol{x}^{g} - \left(\boldsymbol{x}^{g\delta}\right)^T \boldsymbol{K}^{+} \boldsymbol{x}^{g\delta} + \left(\boldsymbol{k}^{-}\right)^T \boldsymbol{x}^{g\delta} \end{aligned} \tag{50}$$

where $\boldsymbol{K}^{+} = diag(\boldsymbol{k}^{+})$. Finally, replacing (37) in (50), we get that the cost incurred by the residential microgrid over the whole time window is equivalent to:

$$\begin{aligned} C\left(\boldsymbol{x}^{g\delta}, \boldsymbol{x}^{a}\right) = \left(\boldsymbol{x}^{a} + \sum_{p=1}^{P} \boldsymbol{d}_p\right)^T \boldsymbol{K}^{+} \left(\boldsymbol{x}^{a} + \sum_{p=1}^{P} \boldsymbol{d}_p\right) \\ -\left(\boldsymbol{x}^{g\delta}\right)^T \boldsymbol{K}^{+} \boldsymbol{x}^{g\delta} + \left(\boldsymbol{k}^{-}\right)^T \boldsymbol{x}^{g\delta}. \end{aligned} \tag{51}$$

IV. Deterministic Formulation of the Scheduling Problem

In the preliminary deterministic model, uncertainty is disregarded and the scheduling problem is solved based on nominal forecasted values. We first formulate the problem aiming at determining the cost-optimal energy scheduling of the users' CLs, HPs, and EVs, ESS charging/discharging profile, and buying/selling strategies:

$$\min_{\substack{\boldsymbol{x}^{l}, \boldsymbol{x}^{p}, \boldsymbol{x}^{v}, \boldsymbol{x}^{v\delta}, \boldsymbol{x}^{s}, \boldsymbol{x}^{s\delta}, \boldsymbol{x}^{g}, \boldsymbol{x}^{g\delta}, \\ \boldsymbol{x}^{a}, \boldsymbol{\delta}^{v}, \boldsymbol{\delta}^{s}, \boldsymbol{\delta}^{g}}} C\left(\boldsymbol{x}^{g\delta}, \boldsymbol{x}^{a}\right) \tag{52}$$

s.t. (1)-(7), (9)-(11), (14)-(20), (22)-(24),

(27)-(33), (36)-(38), (40), (43)-(48).

Problem (52) is called *nominal scheduling*. It is convenient rewriting (52) into a reduced form omitting superfluous terms as follows. First, we note that the objective function (51) contains terms not depending on decision variables, which can be thus neglected. To this aim we transform (51) as follows:

$$\begin{aligned} C\left(\boldsymbol{x}^{g\delta}, \boldsymbol{x}^{a}\right) = \boldsymbol{x}^{aT} \boldsymbol{K}^{+} \boldsymbol{x}^{a} + 2\left(\sum_{p=1}^{P} \boldsymbol{d}_p\right)^T \boldsymbol{K}^{+} \boldsymbol{x}^{a} - \\ \left(\boldsymbol{x}^{g\delta}\right)^T \boldsymbol{K}^{+} \boldsymbol{x}^{g\delta} + \left(\boldsymbol{k}^{-}\right)^T \boldsymbol{x}^{g\delta} + \left(\sum_{p=1}^{P} \boldsymbol{d}_p\right)^T \boldsymbol{K}^{+} \left(\sum_{p=1}^{P} \boldsymbol{d}_p\right) \\ = c\left(\boldsymbol{x}^{g\delta}, \boldsymbol{x}^{a}\right) + \left(\sum_{p=1}^{P} \boldsymbol{d}_p\right)^T \boldsymbol{K}^{+} \left(\sum_{p=1}^{P} \boldsymbol{d}_p\right) \end{aligned} \tag{53}$$

where in the last member of (53) we incorporate all the terms depending only on decision variables in $c\left(\boldsymbol{x}^{g\delta}, \boldsymbol{x}^{a}\right) \triangleq \boldsymbol{x}^{aT} \boldsymbol{K}^{+} \boldsymbol{x}^{a} + 2\left(\sum_{p=1}^{P} \boldsymbol{d}_p\right)^T \boldsymbol{K}^{+} \boldsymbol{x}^{a} - \left(\boldsymbol{x}^{g\delta}\right)^T \boldsymbol{K}^{+} \boldsymbol{x}^{g\delta} + \left(\boldsymbol{k}^{-}\right)^T \boldsymbol{x}^{g\delta}$ and we leave out all the terms depending on optimization input parameters.

Second, we note that equality constraints (37) can be removed. Indeed, replacing (37) in (38) and (43)-(48), variables vector $\boldsymbol{x}^{g}$ can be omitted.

Summing up, the deterministic energy scheduling problem is reformulated as follows:

$$\min_{\substack{\boldsymbol{x}^{l}, \boldsymbol{x}^{p}, \boldsymbol{x}^{v}, \boldsymbol{x}^{v\delta}, \boldsymbol{x}^{s}, \boldsymbol{x}^{s\delta}, \boldsymbol{x}^{g\delta}, \\ \boldsymbol{x}^{a}, \boldsymbol{\delta}^{v}, \boldsymbol{\delta}^{s}, \boldsymbol{\delta}^{g}}} c\left(\boldsymbol{x}^{g\delta}, \boldsymbol{x}^{a}\right) \tag{54}$$

s.t. (1)-(7), (9)-(11), (14)-(20), (22)-(24),

(27)-(33), (36), (40), (47)-(48), and

$$\boldsymbol{x}^{a} + \sum_{p=1}^{P} \boldsymbol{d}_p \le \overline{\boldsymbol{g}} \tag{55}$$

$$\boldsymbol{x}^{a} + \sum_{p=1}^{P} \boldsymbol{d}_p \ge \underline{\boldsymbol{g}} \tag{56}$$

$$\boldsymbol{x}^{a} + \overline{\boldsymbol{g}} \circ \boldsymbol{\delta}^{g} + \sum_{p=1}^{P} \boldsymbol{d}_p \le \overline{\boldsymbol{g}} \tag{57}$$

$$\boldsymbol{x}^{a} - \underline{\boldsymbol{g}} \circ \boldsymbol{\delta}^{g} + \sum_{p=1}^{P} \boldsymbol{d}_p \ge \boldsymbol{0}_{H,1} \tag{58}$$

$$\boldsymbol{x}^{a} - \boldsymbol{x}^{g\delta} + \underline{\boldsymbol{g}} \circ \boldsymbol{\delta}^{g} + \sum_{p=1}^{P} \boldsymbol{d}_p \ge \underline{\boldsymbol{g}} \tag{59}$$

$$\boldsymbol{x}^{a} - \boldsymbol{x}^{g\delta} + \overline{\boldsymbol{g}} \circ \boldsymbol{\delta}^{g} + \sum_{p=1}^{P} \boldsymbol{d}_p \le \overline{\boldsymbol{g}} \tag{60}$$

Note that in the argument of (54) we disregard all the constant terms of the energy cost (53) depending on optimization input parameters, and we replace (38) and (43)-(46) with (55)-(56) and (57)-(60), respectively.

Problem (54)-(60) is a non-convex optimization problem that consists in determining the $4H(N+1)$ real decision variables in $\boldsymbol{x}^{l}, \boldsymbol{x}^{p}, \boldsymbol{x}^{v}, \boldsymbol{x}^{v\delta}, \boldsymbol{x}^{s}, \boldsymbol{x}^{s\delta}, \boldsymbol{x}^{g\delta}, \boldsymbol{x}^{a}$ and $H(N+2)$ binary decision variables in $\boldsymbol{\delta}^{v}, \boldsymbol{\delta}^{s}, \boldsymbol{\delta}^{g}$, which minimize the objective function in (54) and meet the $2H(6N+1)$ bounding constraints (1), (5), (7), and (55)-(56), the $(3HN + 2N + 2H + 1)$ equality constraints (2)-(3), (6), (9), (20), (22), (33), and (36), the $2H(5N+16)$ inequality constraints (4), (14)-(19), (23), (27)-(32), (38), (47)-(48), and (57)-(60), and the $H(N+2)$ integrality constraints (11), (24), and (40). In particular, (54)-(60) is a MIQP problem.

V. Robust Formulation of the Scheduling Problem

The previously defined deterministic scheduling problem unrealistically assumes perfect knowledge of users' energy demand and RES generation (i.e., $\boldsymbol{d}_p$, $p \in \mathcal{P}$). However, the variation in the forecast profile of the NCLs' consumption and RESs generation may cause too much deviation from the optimum in the obtained results, leading to an ineffective scheduling. Here, in order to tackle the users' behavior uncertainty, we firstly define the uncertainty set, then reformulate the problem into its robust counterpart.

A. Data Uncertainty Set of Users' Behavior

Denoting the column vector of parameters related to the pth source of uncertainty (i.e., the NCL consumption profile of each user $n \in \mathcal{N}$ or the produced energy profile of each individual and shared RES $m \in \mathcal{M}$) as $\tilde{\boldsymbol{d}}_p \triangleq \left[\tilde{d}_p(1); \dots; \tilde{d}_p(h); \dots; \tilde{d}_p(H)\right]$, we assume a symmetric distribution for all the uncertain parameters $\tilde{d}_p(h)$ ($h \in \mathcal{H}, p \in \mathcal{P}$):

$$\boldsymbol{d}_p - \hat{\boldsymbol{d}}_p \le \tilde{\boldsymbol{d}}_p \le \boldsymbol{d}_p + \hat{\boldsymbol{d}}_p, p \in \mathcal{P} \tag{61}$$

where $\boldsymbol{d}_p$ is the previously defined vector of nominal values and $\hat{\boldsymbol{d}}_p \triangleq \left[\hat{d}_p(1), \dots, \hat{d}_p(h), \dots, \hat{d}_p(H)\right]$ $(p \in \mathcal{P})$ is the vector collecting the semi-amplitude of maximum variations related to the profile of the pth source of uncertainty. Based on (35), we get that:

$$\hat{\boldsymbol{d}}_p = \begin{cases} \hat{\boldsymbol{b}}_p \text{ if } p \in [1, N] \\ \hat{\boldsymbol{r}}_{p-N} \text{ if } p \in [N+1, P] \end{cases}, p \in \mathcal{P} \tag{62}$$

where $\hat{\boldsymbol{b}}_n$ and $\hat{\boldsymbol{r}}_m$ is the vector of semi-amplitudes related to the energy profile of the nth user's NCL and the mth RES, respectively. We assume that these semi-amplitudes are available based on historical data. Detailed forecast algorithms will not be discussed here since they are beyond the scope of this paper.

Rather than protecting the microgrid against the worst-case deviation of all the parameters, we adopt the cardinality-constrained uncertainty method [35] that allows to decide the level of conservativeness and is able to withstand parameters' uncertainty without excessively affecting the objective function and constraints. We define a non-negative parameter Γ_0 (not necessarily integer) as the budget of uncertainty. This is a robustness factor that denotes the number of parameters (i.e., $d_p(h), n \in \mathcal{P}, h \in \mathcal{H}$) protected against disturbances, taking values in $[0,\ PH]$. The problem solution is guaranteed to be feasible if no more than $\lfloor \Gamma_0 \rfloor$ of the parameters $\tilde{d}_p(h)$ are subject to uncertainty, and one $\tilde{d}_p(h)$ changes no more than $(\lfloor \Gamma_0 \rfloor - \Gamma_0)\hat{d}_p(h)$. Note that $\lfloor \cdot \rfloor$ denotes the ceiling operator: given the real number a, $\lfloor a \rfloor$ is the greatest integer less than or equal to a.

B. Robust Counterpart of the Scheduling Problem

The robust counterpart of the scheduling problem is aimed at achieving a problem formulation that is feasible for any realization of the uncertainty within the defined uncertainty set. Here, uncertainty affects both the objective function in (54) and the inequality constraints in (55)-(60) of the energy scheduling formulated in the previous section. Moreover, we remark that uncertainty not only affects the LHS of inequality constraints, but also their RHS.

Getting inspiration from the cardinality-constrained approach proposed in [35], the robust counterpart of the deterministic scheduling formulation (54)-(60) is given by the following non-linear optimization problem:

$$\min_{\substack{\boldsymbol{x}^l, \boldsymbol{x}^p, \boldsymbol{x}^v, \boldsymbol{x}^{v\delta}, \boldsymbol{x}^s, \boldsymbol{x}^{s\delta}, \boldsymbol{x}^{g\delta}, \\ \boldsymbol{x}^a, \boldsymbol{\delta}^v, \boldsymbol{\delta}^s, \boldsymbol{\delta}^g}} c\left(\boldsymbol{x}^{g\delta}, \boldsymbol{x}^a\right) + \beta(\boldsymbol{x}^a, \Gamma_0) \tag{63}$$

s.t. (1)-(7), (9)-(11), (14)-(20), (22)-(24),

(27)-(33), (36), (40), (47)-(48), and

$$x^a(h) + \sum\nolimits_{p \in \mathcal{P}} d_p(h) + \gamma_h(\Gamma_0) \le \overline{g}(h),\ h \in \mathcal{H} \tag{64}$$

$$x^a(h) + \sum\nolimits_{p \in \mathcal{P}} d_p(h) - \gamma_h(\Gamma_0) \ge \overline{g}(h),\ h \in \mathcal{H} \tag{65}$$

$$x^a(h) + \overline{g}(h)\delta^g(h) + \sum\nolimits_{p=1}^{P} d_p(h) + \gamma_h(\Gamma_0) \le \overline{g}(h),\ h \in \mathcal{H} \tag{66}$$

$$x^a(h) - \underline{g}(h)\delta^g(h) + \sum\nolimits_{p=1}^{P} d_p(h) - \gamma_h(\Gamma_0) \ge 0,\ h \in \mathcal{H} \tag{67}$$

$$x^a(h) - x^{g\delta}(h) + \underline{g}(h)\delta^g(h) + \sum\nolimits_{p=1}^{P} d_p(h) - \gamma_h(\Gamma_0) \ge \underline{g}(h),\ h \in \mathcal{H} \tag{68}$$

$$x^a(h) - x^{g\delta}(h) + \overline{g}(h)\delta^g(h) + \sum\nolimits_{p=1}^{P} d_p(h) + \gamma_h(\Gamma_0) \le \overline{g}(h),\ h \in \mathcal{H} \tag{69}$$

where $\beta(\boldsymbol{x}^a, \Gamma_0)$ is the protection function of the objective function, and $\gamma_h(\Gamma_0)$ $(h \in \mathcal{H})$ are the protection functions of the inequality constraints. For a given solution of (63)-(69), the above introduced $(H+1)$ protection functions are defined as follows:

$$\beta(\boldsymbol{x}^{a*}, \Gamma_0) = \max_{\substack{\mathcal{Q}_1 \cup \{q_1\}, \dots, \\ \mathcal{Q}_H \cup \{q_H\}, \\ \Gamma_1, \dots, \Gamma_H}} 2 \sum\nolimits_{h \in \mathcal{H}} \Big(k^+(h) |x^{a*}(h)| \sum\nolimits_{p \in \mathcal{Q}_h} \hat{d}_p(h) + (\Gamma_h - \lfloor \Gamma_h \rfloor) k^+(h) |x^{a*}(h)| \hat{d}_{q_h}(h) \Big) \tag{70}$$

$$\boldsymbol{\gamma}(\Gamma_0) \triangleq \begin{bmatrix} \gamma_1(\Gamma_0) \\ \vdots \\ \gamma_H(\Gamma_0) \end{bmatrix} = \max_{\substack{\mathcal{Q}_1 \cup \{q_1\}, \\ \dots, \\ \mathcal{Q}_H \cup \{q_H\}, \\ \Gamma_1, \dots, \Gamma_H}} \begin{bmatrix} \sum_{p \in \mathcal{Q}_1} \hat{d}_p(1) + (\Gamma_1 - \lfloor \Gamma_1 \rfloor)\hat{d}_{q_1}(1) \\ \vdots \\ \sum_{p \in \mathcal{Q}_H} \hat{d}_p(H) + (\Gamma_H - \lfloor \Gamma_H \rfloor)\hat{d}_{q_H}(H) \end{bmatrix} \tag{71}$$

$$\text{s.t. } \mathcal{Q}_h \subseteq \mathcal{P}, |\mathcal{Q}_h| = \lfloor \Gamma_h \rfloor, q_h \in \mathcal{P} \backslash \mathcal{Q}_h, h \in \mathcal{H} \tag{72}$$

$$0 \le \Gamma_h \le P, h \in \mathcal{H}, \sum\nolimits_{h \in \mathcal{H}} \Gamma_h = \Gamma_0. \tag{73}$$

where we introduce H supporting variables $\Gamma_1, \dots, \Gamma_h, \dots, \Gamma_H$ to quantify the portions (not necessarily integer) of the total uncertainty budget Γ_0 over all the time slots (see Fig. 2). In (70)-(73) we also introduce H subsets $\mathcal{Q}_1, \dots, \mathcal{Q}_h, \dots, \mathcal{Q}_H$ and H indices $q_1, \dots, q_h, \dots, q_H$ to deal with uncertainty. In particular, $\mathcal{Q}_h \subseteq \mathcal{P}$ (with $h \in \mathcal{H}$) is the subset of uncertainty sources p defined by (62), whose value in time slot h gets the maximum variation (i.e., $d_p(h) + \hat{d}_p(h)$). At most $\lfloor \Gamma_h \rfloor$ uncertainty sources are assumed to belong to this subset. Further, in case Γ_h is not integer, an uncertainty source q_h is selected at each time slot h, whose value is affected by a variation lower than the maximum deviation (i.e., the value is between $d_{q_h}(h)$ and $d_{q_h}(h) + \hat{d}_{q_h}(h)$). For a given time slot h, all the remaining uncertainty sources p not belonging to $\mathcal{Q}_h$ and different from q_h get the nominal values (i.e., $d_p(h)$). As a result, in (63)-(69) robustness is taken into account considering the maximum variation for each uncertainty parameters over the whole time horizon, given the allocation $\Gamma_1, \dots, \Gamma_h, \dots, \Gamma_H$ of the total uncertainty budget Γ_0 over all the time slots.

Further details on the above-defined robust counterpart (63)-(69) and the differences with the approach proposed in [35] are provided in Appendix A.

C. Reformulation of the Robust Counterpart

Observing (63) to (69), it can be found that the robust counterpart of the scheduling problem includes strong non-linearities and cardinality calculations due to the inner maximization defined by (70)-(73) and placed in (63)-(69). Thus, it is still difficult to solve the problem in its current min-max form. This can be resolved by transforming the robust counterpart into an easier form. By introducing further supporting variables $\boldsymbol{y}$,$\Lambda, \lambda, \Theta_{ph}, \boldsymbol{\theta}_{ph}$ (with $p \in \mathcal{P}, h \in \mathcal{H}$) and taking advantage of the strong duality theorem [55], we transform (63)-(69) into an equivalent MIQP formulation as follows:

$$\min_{\substack{\boldsymbol{x}^l,\boldsymbol{x}^p,\boldsymbol{x}^v,\boldsymbol{x}^{v\delta},\boldsymbol{x}^s,\boldsymbol{x}^{s\delta},\boldsymbol{x}^{g\delta},\\ \boldsymbol{x}^a,\boldsymbol{\delta}^v,\boldsymbol{\delta}^s,\boldsymbol{\delta}^g,\\ \boldsymbol{y},\Lambda,\boldsymbol{\lambda},\\ \Theta_{11},\dots,\Theta_{1H},\dots,\Theta_{P1},\dots,\Theta_{PH},\\ \boldsymbol{\theta}_{11},\dots,\boldsymbol{\theta}_{1H},\dots,\boldsymbol{\theta}_{P1},\dots,\boldsymbol{\theta}_{PH}}} c(\boldsymbol{x}^{gu},\boldsymbol{x}^a) + \Gamma_0\Lambda + \sum_{p\in\mathcal{P}}\sum_{h\in\mathcal{H}}\Theta_{ph} \tag{74}$$

s.t. (1)-(7), (9)-(11), (14)-(20), (22)-(24), (27)-(33), (36), (38), (40), (47)-(48), and

$$\boldsymbol{x}^a + \sum_{p=1}^{P}\boldsymbol{d}_p + \Gamma_0\boldsymbol{\lambda} + \sum_{p\in\mathcal{P}}\sum_{h\in\mathcal{H}}\boldsymbol{\theta}_{ph} \le \overline{\boldsymbol{g}} \tag{75}$$

$$\boldsymbol{x}^a + \sum_{p=1}^{P}\boldsymbol{d}_p - \Gamma_0\boldsymbol{\lambda} - \sum_{p\in\mathcal{P}}\sum_{h\in\mathcal{H}}\boldsymbol{\theta}_{ph} \ge \underline{\boldsymbol{g}} \tag{76}$$

$$\boldsymbol{x}^a + \overline{\boldsymbol{g}}\circ\boldsymbol{\delta}^g + \sum_{p=1}^{P}\boldsymbol{d}_p + \Gamma_0\boldsymbol{\lambda} + \sum_{p\in\mathcal{P}}\sum_{h\in\mathcal{H}}\boldsymbol{\theta}_{ph} \le \overline{\boldsymbol{g}} \tag{77}$$

$$\boldsymbol{x}^a - \underline{\boldsymbol{g}}\circ\boldsymbol{\delta}^g + \sum_{p=1}^{P}\boldsymbol{d}_p - \Gamma_0\boldsymbol{\lambda} - \sum_{p\in\mathcal{P}}\sum_{h\in\mathcal{H}}\boldsymbol{\theta}_{ph} \ge \boldsymbol{0}_{H,1} \tag{78}$$

$$\boldsymbol{x}^a - \boldsymbol{x}^{g\delta} + \underline{\boldsymbol{g}}\circ\boldsymbol{\delta}^g + \sum_{p=1}^{P}\boldsymbol{d}_p - \Gamma_0\boldsymbol{\lambda} - \sum_{p\in\mathcal{P}}\sum_{h\in\mathcal{H}}\boldsymbol{\theta}_{ph} \ge \underline{\boldsymbol{g}} \tag{79}$$

$$\boldsymbol{x}^a - \boldsymbol{x}^{g\delta} + \overline{\boldsymbol{g}}\circ\boldsymbol{\delta}^g + \sum_{p=1}^{P}\boldsymbol{d}_p + \Gamma_0\boldsymbol{\lambda} + \sum_{p\in\mathcal{P}}\sum_{h\in\mathcal{H}}\boldsymbol{\theta}_{ph} \le \overline{\boldsymbol{g}} \tag{80}$$

$$w_0\Lambda + \boldsymbol{w}^T\boldsymbol{\lambda} \ge 0 \tag{81}$$

$$w_0\Theta_{ph} + \boldsymbol{w}^T\boldsymbol{\theta}_{ph} \ge 0, p \in \mathcal{P}, h \in \mathcal{H} \tag{82}$$

$$w_0\left(\Lambda + \Theta_{ph}\right) + \boldsymbol{w}^T\left(\boldsymbol{\lambda} + \boldsymbol{\theta}_{ph}\right) \ge w_0 2k^+(h)\hat{d}_p(h)y(h) + \boldsymbol{w}^T\widehat{\boldsymbol{d}}_p, \quad p \in \mathcal{P}, h \in \mathcal{H} \tag{83}$$

$$-\boldsymbol{y} \le \boldsymbol{x}^a \le \boldsymbol{y}. \tag{84}$$

where w_0 is the non-negative weight associated to the protection function of the objective and $\boldsymbol{w} \triangleq [w_1; \dots; w_H]$ is a column vector collecting the non-negative weights associated to the protection function of the inequality constraints.

A detailed description of the introduced supporting variables and a comprehensive proof of the robust counterpart reformulation are provided in Appendix B.

We finally remark that (74)-(84) is a MIQP problem that consists in determining the $(H(P(H+1)+4N+6)+1)$ real and $H(N+2)$ binary decision variables, which minimize the objective function in (74) and meet the $12HN$ bounding constraints (1), (5), and (7), the $(3HN+2N+2H+1)$ equality constraints (2)-(3), (6), (9), (20), (22), (33), and (36), the $2H(5N+16)$ inequality constraints (4), (14)-(19), (23), (27)-(32), (38), (47)-(48), and (77)-(84), and the $H(N+2)$ integrality constraints (11), (24), and (40).

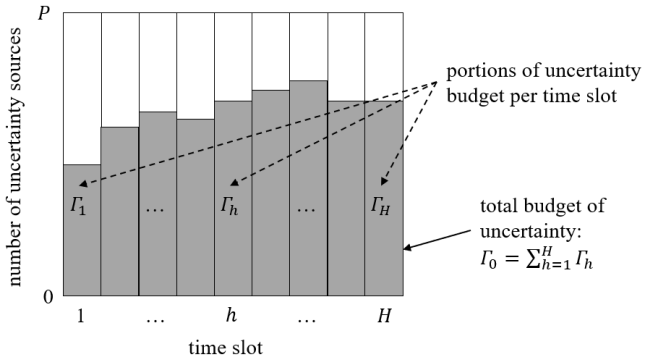

Fig. 2. Illustration of the allocation of the total uncertainty budget over time slots.

D. The Robust Control Solution Based on Budget of Uncertainty

Solving the transformed robust counterpart (74)-(84), the energy scheduling can be obtained with different robustness levels. Indeed, the robustness of the energy scheduling varies with the total budget of uncertainty (Γ_0). Here, the role of Γ_0 is to adjust the robustness of the proposed scheduling method against the level of conservativeness of the solution. Accordingly, the conservativeness of the solution can be controlled. Note that for $\Gamma_0 = 0$, $\beta(\boldsymbol{x}^a, \Gamma_0) = 0$ and $\gamma_h(\Gamma_0) = 0$ ($h \in \mathcal{H}$), the constraints are equivalent to those of the deterministic problem. In this case, the total cost is minimum but the results are too optimistic. Likewise, for $\Gamma_0 = PH$, the uncertainty is fully addressed during the operation, but the solution is obtained in the most conservative case (i.e., the worst case over all the possible realization of uncertain parameters). Thus, by varying $\Gamma_0 \in [0, PH]$, a flexibility is provided for the decision maker to adjust the robustness of the method against the level of conservativeness and a trade-off between users' energy payment and constraint violation rate is found. In the subsequent case study, we show that even in the case of higher number of changes than Γ_0, the robust solution is feasible with very high probability. The conservativeness of the solution and the maximum probability of constraint violation under the given uncertainty bounds can be controlled by adjusting the value of the budget of uncertainty [35].

VI. Simulation Results and Analysis

In this section, we provide a day-ahead energy scheduling on a weekday for a residential microgrid to evaluate the performance of the proposed robust framework. We investigate the effects of the proposed method on: 1) the users' energy payment, 2) the constraint violation rate, and 3) the PAR in exchanged energy. Note that the PAR in exchanged energy can be defined as in [16]:

$$PAR = \max_{h\in\mathcal{H}}|x^g(h)| \Big/ \frac{1}{H}\sum_{h=1}^{H}x^g(h). \tag{85}$$

The problem is solved by CPLEX 12.8 in MATLAB R2017a on a desktop PC with an Intel i7-7500U core processor with 2.70 GHz (4 CPUs) and 12 GB RAM memory.

A. Parameters and Settings

The sample power system (see Fig. 1) has $N = 10$ smart users subscribing to the EMS. For simplicity, we assume that each user consists of a CL, a NCL, and a PEV, while all users share an ESS, a PVS and a DWT. We consider the time window for simulation of one day from 0:00 to 23:59. Each time slot is set equal to one hour, meaning that the decision is made by solving the optimization problem for the next $H = 24$ hours. As mentioned in Section III, we assume that, in the cost function, the term corresponding to the electricity bought from the power grid is quadratic, while the related term to the electricity sold back to the power grid is linear. The price signals for bought and sold electrical energy throughout the day are taken from [16], [56], [57]. Accordingly, the daily cost coefficients for the energy bought from the power grid during peak-demand time slots (i.e., [9:00 to 11:00] and [16:00 to 21:00]) and off-peak-demand time slots (i.e., [0:00 to 8:00], [12:00 to 15:00] and [22:00 to 24:00]) are set to 0.1875 ¢/kWh^2 and 0.0937 ¢/kWh^2 respectively. Also, the cost coefficients for energy sold to the power grid for peak-demand and off-peak-demand time slots are considered as 0.1188 ¢/kWh and 0.0594 ¢/kWh respectively. Figure 3 shows both the buying and selling cost coefficient profiles. We assume that the maximum permissible energy transferred with the power grid (both for buying and selling) for all time slots is 60 kWh. The energy required by the energy-based CLs ranges from 0 to 3.5 kWh. We assume that the cumulative daily energy demand for each user's CL is 30 kWh. To model the users' NCLs, we use the actual profiles of average hourly electricity consumption for a sample of homes in Italy taken from [58]. The aggregated forecast energy demand profile of NCLs over all users (i.e., $\sum_{n=1}^{N} \boldsymbol{b}_n$) and the corresponding uncertainty range (that is 10% of the forecast value for each time slot) is presented in Fig. 4. We consider a shared ESS unit with maximum storage capacity 120 kWh, and with the maximum charging/discharging rate of 25 kWh. We assume that both charging and discharging efficiencies are 0.9, initial charge level is zero, and battery degradation and leakage effects are negligible. The hybrid forecast energy generation profile of the shared PVS and DWT, taken from [59], with corresponding uncertainty range (that is 10% of the forecast value for each time slot), is represented in Fig. 5. It is to be noted that, as the energy generation profiles of the RESs depend on weather conditions, we assume that the hybrid forecast energy generation profile of individual RESs for each user is obtained scaling by 10% the shared PVS and DWT profile (i. e., Fig. 5) and considering a 10% uncertainty range for each time slot. For each PEV, we assume that the initial battery charge level and the desired final state of charge are 1 and 5 kWh, respectively. Also, we assume that the PEV leaves home at 8:00 and returns at 18:00. That is, the PEV is plugged-in during time slots [0:00, 08:00] ∪ [18:00, 24:00] and can participate in the energy scheduling (e.g., release its remaining stored energy to the system after arrival). We adopt discrete Gaussian distributed random variables to model the uncertainties of NCLs and RESs. We also assume that users are equipped with identical HVAC systems (i.e., HPs) and the desired indoor temperature setpoint ranges in [18, 21] ℃. Moreover, we consider active setpoints during time slots [06:00, 8:00] ∪ [17:00, 24:00], that is when occupants are present. We set a desired temperature at 19℃ upon the nominal arrival time of occupants (i. e., 18:00), and the HP can start running earlier (e. g., 17:00) to raise the temperature to the desired value. We take the profile of daily outdoor temperature for a typical winter day in Italy from [58], and we set the value of model parameters as $\tau_n = 3600$ s, $\pi_n = 15\ {}^{W\,s}/_{m}$ and $E_n = 2.5$ kWh.

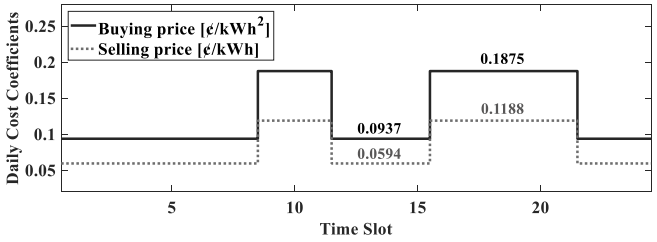

Fig. 3. Daily cost coefficients for the energy bought/sold from/to the power grid during peak-demand and off-peak-demand time slots..

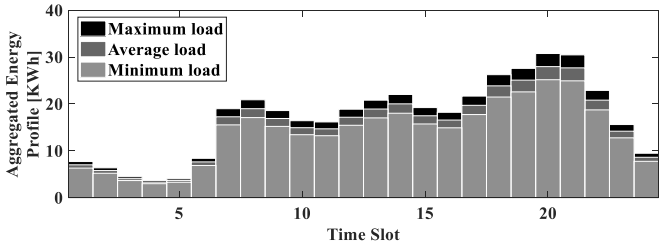

Fig. 4. Aggregated forecast energy demand profile of NCLs with corresponding uncertainty ranges.

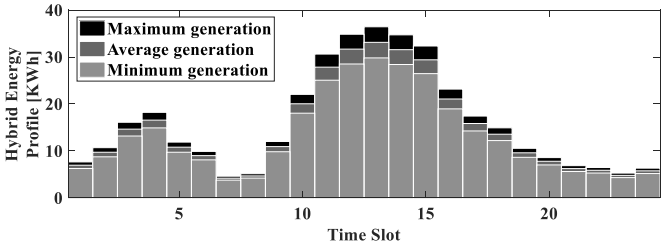

Fig. 5. Hybrid forecast energy generation profiles of shared PVS and DWT with corresponding uncertainty ranges.

B. Results

We simulate the energy scheduling of the sample microgrid by applying the method for three cases of analysis. First, the simulation results are reported and compared in three cases.

Case 1: the nominal model with perfect forecast data ignoring uncertainty (i.e., when $\Gamma = 0$). Therefore, no protection terms are considered against data uncertainty (i.e. $\beta(\boldsymbol{x}^a, \Gamma_0) = 0$ and $\gamma_h(\Gamma_0) = 0, h \in \mathcal{H}$).

Case 2: the robust model considering full protection against data uncertainty (i.e., the worst-case realization) by adopting the maximum budget of uncertainty ($\Gamma_0 = PH = 528$), implying the most conservative solution.

Case 3: the robust model considering uncertainty with $\Gamma_0 = \Gamma_0^*$, where $\Gamma_0^* \in (0, PH)$ corresponds to a potential choice for the budget of uncertainty when the robustness of the solution

rarely changes for $\Gamma_0 > \Gamma_0^*$. This value can be obtained after sensitivity analyses over different budgets of uncertainty (we set $\Gamma_0^* = 104$), meaning that increasing the protection level by choosing $\Gamma_0 > \Gamma_0^*$ does not provide a significant improvement in the robustness of the solution against uncertainty, due to the change in constraint violation for $\Gamma_0 \in [104, 528]$).

The results of the energy scheduling for the three cases are presented in Figs. 6-9. In Fig. 6, the scheduled aggregated energy profiles of the energy-based CLs over users (i.e., $\sum_{n=1}^{N} \boldsymbol{x}_n^l$) are reported. Figure 7 represents the charging/discharging activities of the shared ESS (i.e., $\boldsymbol{x}^s$). Figure 8 shows the optimal aggregated charging/discharging activities of PEVs (i.e., $\sum_{n=1}^{N} \boldsymbol{x}_n^v$). In Fig. 9, the scheduled aggregated energy profiles of the HPs over users (i.e., $\sum_{n=1}^{N} \boldsymbol{x}_n^p$) are reported. First, the results show that the scheduling arranges the operation time of the CLs to the off-peak time slots for minimizing the energy payment. Second, the ability of optimally storing the energy in the off-peak time slots and releasing it during the peak hour periods by the ESS and PEVs effectively contributes to the minimization of the total energy payment. Furthermore, the scheduling tries to exploit the energy harvested from the RESs first for supplying the users' energy demand or charging the ESS and PEVs, and secondarily for transferring surplus energy to the power grid. For this specific scenario, the users' daily energy payments and the PAR values for *cases 1*, *2*, and *3* are respectively 27.81€, 29.98€, and 28.62€ and 2.277, 2.325, and 2.297. Although the solution of *case 1* leads to the minimum daily users' energy payment (7.25% lower than *case 2*, and 2.84% lower than *case 3*) and the lowest PAR (6.61% lower than *case 2*, and 3.11% lower than *case 3*), the result is the most optimistic case since it ignores the effects of the data uncertainty. Therefore, in real conditions, any disturbance in the forecast profiles of the load demands or the RESs energy generation may cause an excessive increase in the obtained value of the objective function. Also, the contractual constraints can be easily violated over the time window in presence of any disturbances because of the lack of any protection term in (38) against data uncertainty.

On the other hand, the solution of *case 2* provides full immunity against the worst-case realization. Here, the worst-case occurs when the energy demand uncertainty takes its upper bound, while the RESs generation uncertainty stands on its lower band during all time slots. This case guarantees that the solution is immunized against all possible uncertain data, leading to zero constraint violation rate. However, this immunity is obtained at the expenses of an unnecessarily too conservative solution, causing the highest users' daily energy payment (i.e., 29.98€) and highest PAR (i.e., 2.613). In order to prevent such a too conservative solution, *case 3* provides a compromise where there is a respective decrease of 4.53% and 1.21% in the users' daily energy payment and the PAR compared to those in the *case 2*. Meanwhile, the solution obtained by *case 3* is robust against data uncertainty with very high probability (i.e., more than 99%) that is discussed in the next subsection. In general, by adjusting the budget of uncertainty in the possible range ($\Gamma_0 \in [0, 528]$), the level of conservativeness of the solution can be controlled and a trade-off between the users' energy payment and the constraint violation rate can be established based on the decision maker's preferences. In the next subsection, we also argue that when the forecast data are subject to uncertainty, the robust model

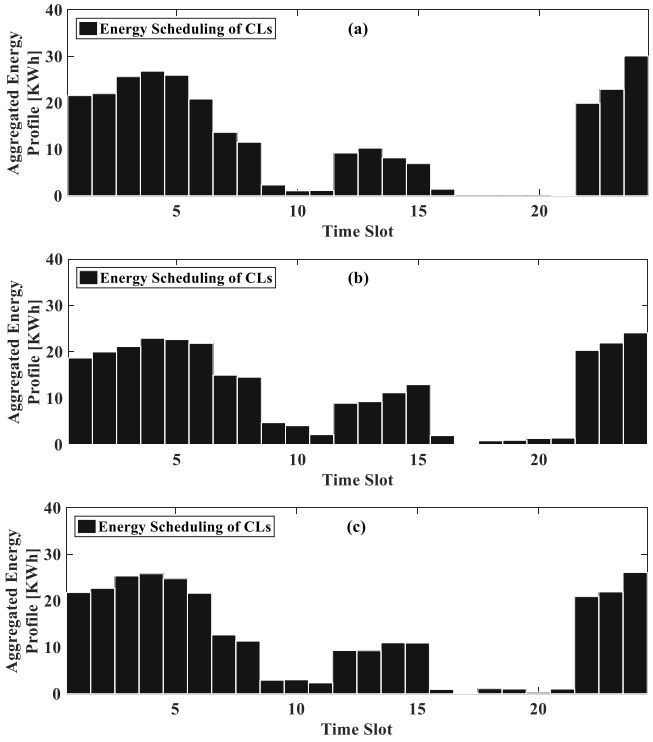

Fig. 6. Aggregated energy profiles of the energy-based CLs for: (a) *case 1*, (b) *case 2*, and (c) *case 3*.

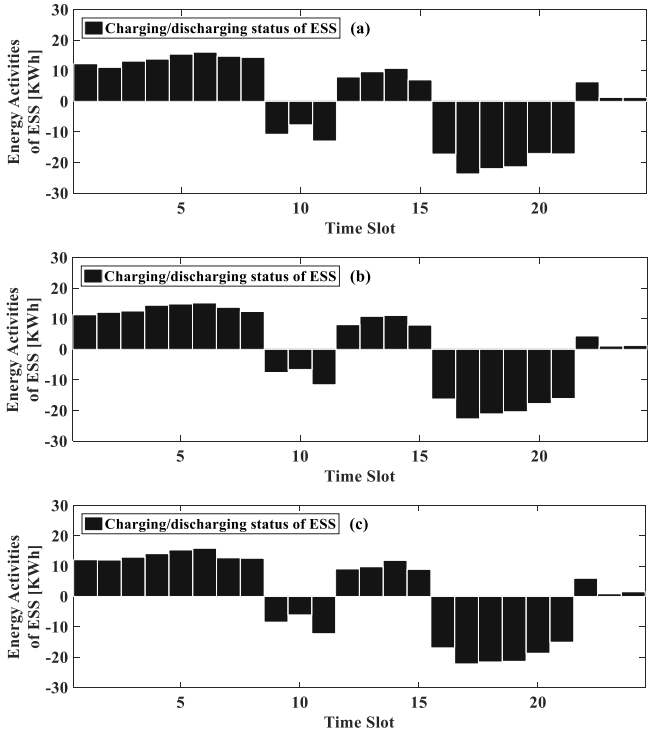

Fig. 7. Charging/discharging strategies of shared ESS for: (a) *case 1*, (b) *case 2*, and (c) *case 3*.

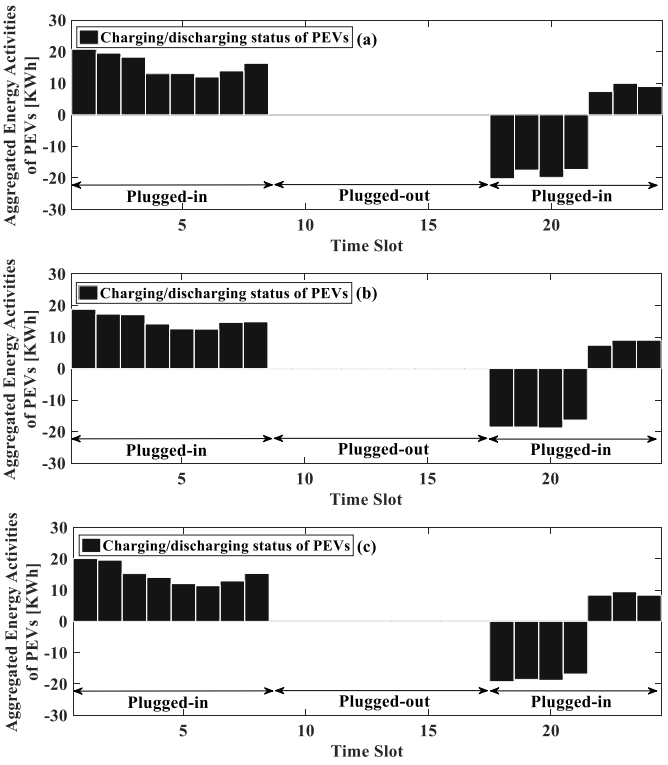

Fig. 8. Aggregated charging/discharging strategies of PEVs for: (a) *case 1*, (b) *case 2*, and (c) *case 3*.

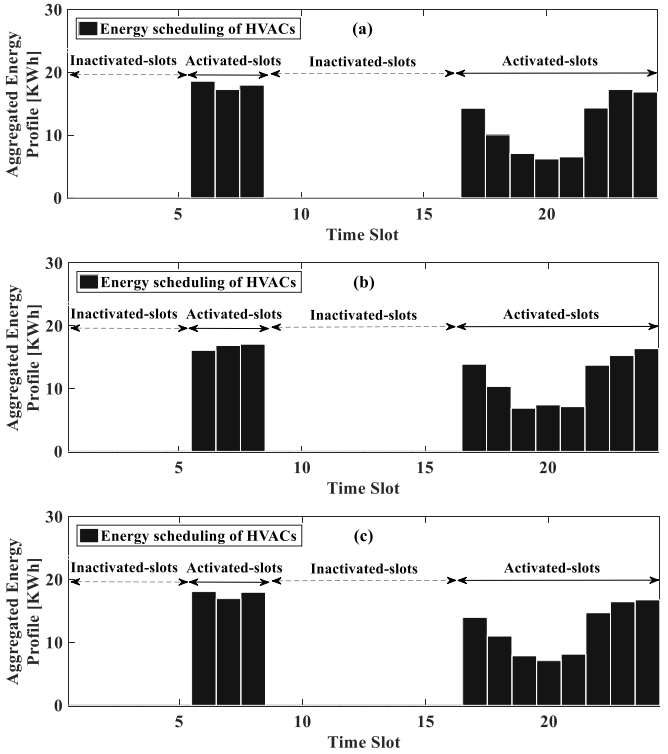

Fig. 9. Aggregated energy profiles of the HPs for: (a) *case 1*, (b) *case 2*, and (c) *case 3*.

provides a good performance in flattening the profile of the total exchanged energy with the power grid, leading to a lower PAR. For a further validation of the results, the method should be also analyzed in real conditions, i.e., evaluating the results achieved for different realizations of uncertain variables, as provided in the next subsection.

C. Discussion

To show the impact of data uncertainty on the problem and demonstrate the effectiveness of the proposed robust approach against it, Monte Carlo (MC) simulations are used to generate 10,000 scenarios for the users' demand and the RESs generation uncertainties. We then present a sensitivity analysis of the protection level with respect to the daily energy payment, the constraint violation rate, and the PAR through comparing the solutions generated by different budgets of uncertainty. The actual profile of the NCLs at each MC iteration is obtained by adding a normally distributed random sequence with zero mean and standard deviation equal to 0.2 kWh to the nominal forecast values. In order to obtain some insights on the effect of changing the budget of uncertainty on the users' energy payment, constraint violation rate and the PAR, and ultimately to show the robustness of the approach, we present the energy scheduling results for the average profile of the MC simulations for all iterations. The profiles of the average energy exchanged with the power grid over all MC iterations compared to the maximum permissible energy bought/sold from/to the power grid per time slot (i.e., $\overline{g}(h)/\underline{g}(h)$), indicated with the dashed line, for *case 1*, *case 2*, and *case 3* are illustrated in Fig. 10a, 10b and 10c, respectively. It can be found that, under the considered scenarios, the energy exchanged between users and the power grid violates constraint (38) in more than 34.83% of time slots in *case 1 (the nominal model)*, which is undesirable (Fig. 11a). Conversely, in *case 2* (*robust model* - worst-case mode), these constraints are fully satisfied, confirming that full protection is established (Fig. 11b). In *case 3* (*the robust model* with $\Gamma_0 = \Gamma_0^* = 104$), the average exchanged energy profile (Fig. 11c) shows that even by adopting a budget of uncertainty less than 20% of the maximum protection level, the constraint (38) over time window is met with very high probability (more than 99%). Table I reports the comparison of the average MC simulation results achieved by the three cases of simulation in terms of the daily total cost, the probability of constraint violation, the PAR, and the so-called *price of robustness* (PoR) defined as the percentage of relative difference between the costs achieved by a robust solution and a nominal solution [35]. We calculate the PoR as:

$$PoR = 100\frac{\sum_{h=1}^{H} C_h(x^{g,rob}(h)) - \sum_{h=1}^{H} C_h(x^{g,nom}(h))}{\sum_{h=1}^{H} C_h(x^{g,nom}(h))} \quad (86)$$

where $x^{g,nom}(h)$ and $x^{g,rob}(h)$ ($h \in \mathcal{H}$) are the optimal values of the energy that the microgrid exchanges with the power grid in accordance with the nominal and the robust scheduling, respectively.

Although in *case 1* a better respective saving of 3.61% and 1.88% in the value of average daily users' energy payment can be achieved compared to those in *case 2* and *case 3*, the constraint violation rate is drastically higher than those in two other cases (i.e., 35.02% and 34.10% higher than the values in the *case 2* and *case 3* respectively). On the other hand, the daily users' energy payment in *case 3* is 1.76% lower than its value in *case 2*. Moreover, the

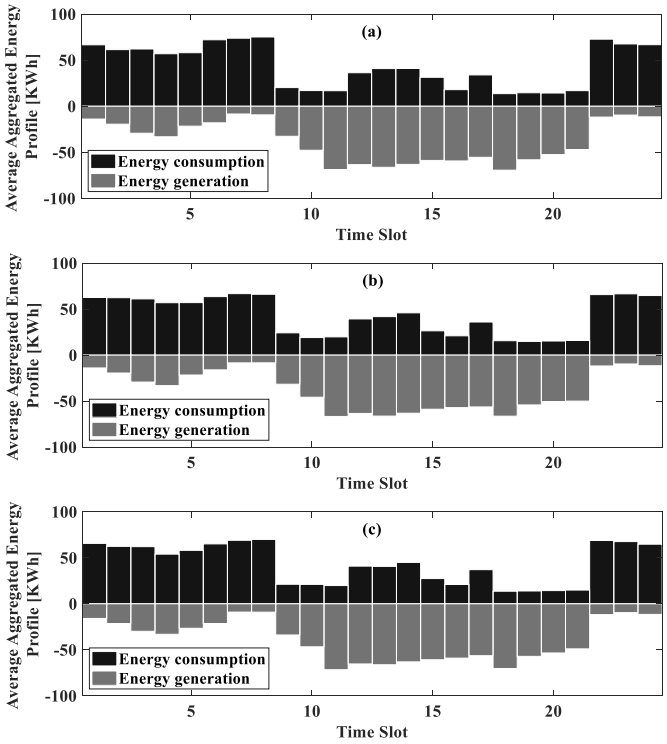

Fig. 10. Average aggregated energy consumed by the microgrid (i.e., NCLs' and CLs' demands, HPs' demand, ESS's charging and PEVs' charging and average energy generated by the microgrid (i.e., shared and individual RESs' generation, ESS's discharging and PEVs' discharging for: (a) *case 1*, (b) *case 2*, and (c) *case 3*.

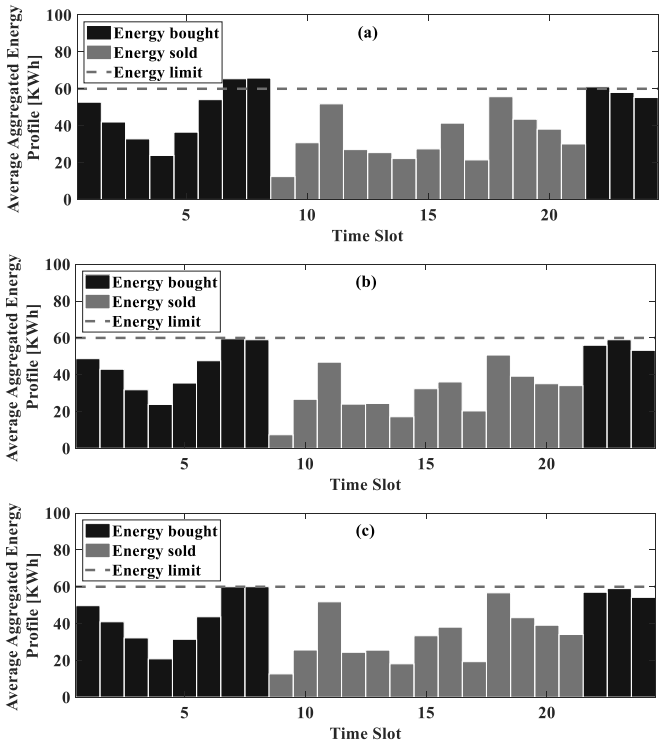

Fig. 11. Average total energy bought/sold from/to the grid versus maximum permissible energy exchanged with the grid for: (a) *case 1*, (b) *case 2*, and (c) *case 3*.

PAR in the total energy exchanged in *case 3* is 1.19% lower than its value in *case 2*. Moreover, the PAR in the total energy exchanged in *case 3* is 1.66% lower than the PAR in *case 2*. Therefore, we can conclude that by selecting $\Gamma_0 = \Gamma_0^*$, we avoid a significant penalty for the objective function value to protect the solution against constraint violation. Hence, the results confirm the importance of suitably selecting the budget of uncertainty for a trade-off between cost and robustness. In addition, the fourth column of Table I reports the average computational runtime in the three scenarios: the computation time for all the simulations is less than 1.5 seconds.

Summing up, the simulation results show that the method allows the decision maker to make a trade-off between constraint violation rate and PoR by adjusting the values of the budget of uncertainty. The robust energy scheduling not only reduces the users' energy bills and the PAR by encouraging users to shift high-load CLs to the off-peak time slots, but also guarantees the solution to satisfy constraints with very high probability in the presence of the demand and the RESs generation uncertainties. The simulation also shows that the proposed robust approach is computationally tractable, with a reasonable computational running time. We remark that the proposed framework is generic and flexible as it can be applied to different structures of microgrids (for example, with multiple CLs, NCLs, PEVs and non-interruptible loads) considering various types of uncertainties in distributed energy generation (e.g., a large number of shared distributed generation resources, which can be included in set $\mathcal{M}$) or demand, appearing in the LHS or RHS of the constraints of the robust counterpart.

D. Comparison with a Related Approach

For the sake of assessment and to better show the advancement of our approach with respect to the related literature, we compare the results of our approach with a well-known existing robust technique. Specifically, we use as reference approach the box-uncertainty-set method, where uncertain parameters are assumed to take their values from different intervals independently (we refer to [60], [61] for more details about the box-uncertainty-set method). We present a sensitivity analysis of the MC simulation results with respect to different budgets of uncertainty for both methods in terms of total energy payment, level of conservativeness, and the PAR of the energy profile, all reported in Figs. 12a-12c. As can be observed from the results, despite the constraint violation rate within the primary time slots for our approach is slightly higher than the box-uncertainty-set method, our method provides a less conservative solution which always exhibits lower daily energy payments and PARs than the box-uncertainty-set method. These results confirm the effectiveness of our approach, enabling the decision maker to make a good trade-off between the total energy payment by users, the level of conservativeness and the PAR by changing the value of the budget of uncertainty.

VII. CONCLUSIONS

This paper proposes a novel adjustable robust energy scheduling framework for residential microgrids comprising energy-based and comfort-based CLs, individual PEVs and RESs, shared ESS and RESs under quadratic/linear dynamic pricing. We focus on uncertainties associated with RES generation and users' energy demand. A MIQP problem is

TABLE I
COMPARISON OF AVERAGE MC SIMULATION* RESULTS

	Daily Users' Payment (€/day)	Constraint violation rate (%)	PAR (%)	PoR (%)	Computational runtime (s)
Case 1	29.11	35.02	2.339	0	1.16
Case 2	30.20	0.00	2.380	3.74	1.48
Case 3	29.67	0.92	2.352	1.92	1.25

* Simulation over 10,000 iterations

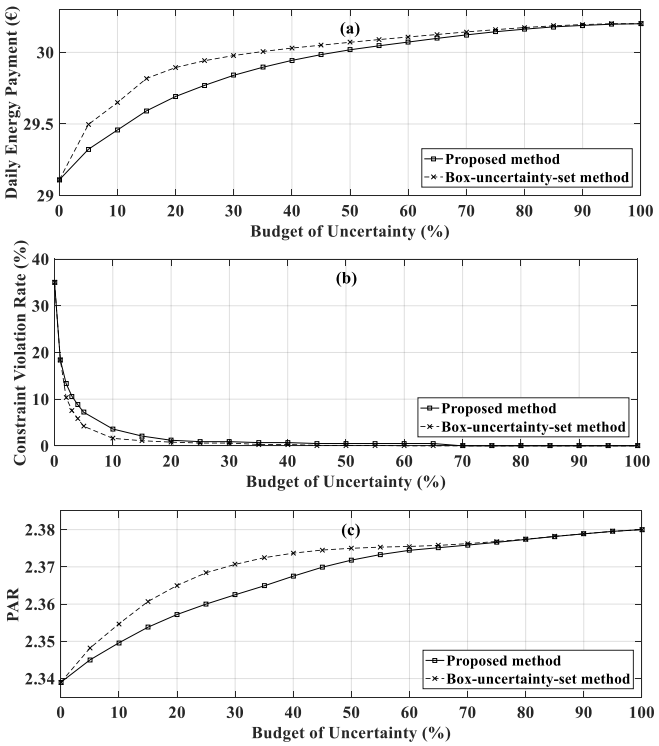

Fig. 12. Sensitivity analysis of the daily energy payment (a), the constraint violation rate (b), and the PAR (c) with respect to different budgets of uncertainty for the proposed method and the robust optimization approach based on box- uncertainty set.

formulated to find the optimal scheduling of CLs as well as charging/discharging strategies of the ESS and PEVs. The simulation results highlight the robustness of the proposed energy scheduling in the uncertain context. A trade-off can be made by the decision maker to resolve the conflict between energy payment minimization and the contractual constraint satisfaction, which is advantageous for both the residential microgrid and the power grid. The future research paths include extending the system model by integrating additional subsystems such as non-interruptible loads, or other types of uncertainty sources such as uncertain real-time pricing and PEV plug-in/out times. Moreover, towards the deployment of large-scale smart grids, the proposed robust scheduling problem can be expanded and resolved in a distributed multi-agent fashion. Future work may also incorporate the robust method with a receding horizon mechanism for real-time energy scheduling.

APPENDIX A

In this appendix, we provide the mathematical steps employed in defining (63)-(69) as the robust counterpart of the scheduling problem (54)-(60).

Preliminarily, for the ease of implementation, following [35], we transform (54)-(60) into an equivalent form where the objective function is not subject to uncertainty, and data uncertainty only affects the elements in the LHS of constraints. In particular, we get an equivalent problem with linear objective function and both quadratic and linear constraints as follows:

$$\min_{\substack{\boldsymbol{x}^l,\boldsymbol{x}^p,\boldsymbol{x}^v,\boldsymbol{x}^{v\delta},\boldsymbol{x}^s,\boldsymbol{x}^{s\delta},\boldsymbol{x}^{g\delta},\\ \boldsymbol{x}^a,\boldsymbol{\delta}^v,\boldsymbol{\delta}^s,\boldsymbol{\delta}^g,\alpha,\boldsymbol{x}^b}} \alpha \tag{87}$$

s.t. (1)-(7), (9)-(11), (14)-(20), (22)-(24),

(27)-(33), (36), (40), (47)-(48), and

$$\boldsymbol{x}^b = \mathbf{1}_{P,1} \tag{88}$$

$$c\left(\boldsymbol{x}^{g\delta}, \boldsymbol{x}^a\right) - \alpha \leq 0 \tag{89}$$

$$\boldsymbol{x}^a + \sum_{p=1}^{P} \boldsymbol{d}_p \circ \boldsymbol{x}_p^b \leq \overline{\boldsymbol{g}} \tag{90}$$

$$\boldsymbol{x}^a + \sum_{p=1}^{P} \boldsymbol{d}_p \circ \boldsymbol{x}_p^b \geq \underline{\boldsymbol{g}} \tag{91}$$

$$\boldsymbol{x}^a + \overline{\boldsymbol{g}} \circ \boldsymbol{\delta}^g + \sum_{p=1}^{P} \boldsymbol{d}_p \circ \boldsymbol{x}_p^b \leq \overline{\boldsymbol{g}} \tag{92}$$

$$\boldsymbol{x}^a - \underline{\boldsymbol{g}} \circ \boldsymbol{\delta}^g + \sum_{p=1}^{P} \boldsymbol{d}_p \circ \boldsymbol{x}_p^b \geq \mathbf{0}_{H,1} \tag{93}$$

$$\boldsymbol{x}^a - \boldsymbol{x}^{g\delta} + \underline{\boldsymbol{g}} \circ \boldsymbol{\delta}^g + \sum_{p=1}^{P} \boldsymbol{d}_p \circ \boldsymbol{x}_p^b \geq \underline{\boldsymbol{g}} \tag{94}$$

$$\boldsymbol{x}^a - \boldsymbol{x}^{g\delta} + \overline{\boldsymbol{g}} \circ \boldsymbol{\delta}^g + \sum_{p=1}^{P} \boldsymbol{d}_p \circ \boldsymbol{x}_p^b \leq \overline{\boldsymbol{g}}. \tag{95}$$

Note that in (87) and (89) we introduce the scalar auxiliary variable α to move the uncertain parameters from objective function to inequality constraints. Similarly, we introduce vector $\boldsymbol{x}^b \triangleq \left[\boldsymbol{x}_1^b; \ldots; \boldsymbol{x}_p^b; \ldots; \boldsymbol{x}_P^b\right]$ collecting P column vectors of H auxiliary variables $\boldsymbol{x}_p^b \triangleq \left[x_p^b(1); \ldots; x_p^b(h); \ldots; x_p^b(H)\right]$ $(p \in \mathcal{P})$ to preserve uncertain parameters in the LHS of constraints.

Assuming that optimization input parameters take the values defined by (62), we first replace the nominal value of the PH parameters $d_p(h)$ $(h \in \mathcal{H}, p \in \mathcal{P})$ with its deviated value $\tilde{d}_p(h)$ in all the minority (89), (90), (92), (94) and majority inequalities (91), (93), (95). Then, getting inspiration from the cardinality-constrained approach proposed in [35], for a fixed $\Gamma_0 \in [0, PH]$, we impose that only a subset of these parameters vary to adversely affect the solution. Finally, for each of the above mentioned constraints, the final mathematical expression is resorted as a summation of two main terms, one related to the deterministic function, and the second called protection function, with all sub-terms including the variation of the uncertain parameter (i.e., $\hat{d}_p(h), h \in \mathcal{H}, p \in \mathcal{P}$).

Summing up, the corresponding robust counterpart of the deterministic formulation (87)-(95) is given by the following non-linear optimization problem:

$$\min_{\substack{\boldsymbol{x}^l,\boldsymbol{x}^p,\boldsymbol{x}^v,\boldsymbol{x}^{v\delta},\boldsymbol{x}^s,\boldsymbol{x}^{s\delta},\boldsymbol{x}^{g\delta},\\ \boldsymbol{x}^a,\boldsymbol{\delta}^v,\boldsymbol{\delta}^s,\boldsymbol{\delta}^g,\alpha,\boldsymbol{x}^b}} \alpha \tag{96}$$

s.t. (1)-(7), (9)-(11), (14)-(20), (22)-(24),

(27)-(33), (36), (40), (47)-(48), and

$$c\left(\boldsymbol{x}^{g\delta}, \boldsymbol{x}^{a}\right) - \alpha + \beta(\boldsymbol{x}^{a}, \Gamma_0) \leq 0 \quad (97)$$

$$\sum_{p\in\mathcal{P}} d_p(h)\, x_p^b(h) + x^a(h) + \gamma_h(\boldsymbol{x}^b, \Gamma_0) \leq \overline{g}(h), h \in \mathcal{H} \quad (98)$$

$$\sum_{p\in\mathcal{P}} d_p(h)\, x_p^b(h) + x^a(h) - \gamma_h(\boldsymbol{x}^b, \Gamma_0) \geq \overline{g}(h), h \in \mathcal{H} \quad (99)$$

$$\begin{aligned} x^a(h) + \overline{g}(h)\delta^g(h) + \textstyle\sum_{p=1}^{P} d_p(h) x_p^b(h) \\ +\gamma_h(\boldsymbol{x}^b, \Gamma_0) \leq \overline{g}(h), h \in \mathcal{H} \end{aligned} \quad (100)$$

$$\begin{aligned} x^a(h) - \underline{g}(h)\delta^g(h) + \textstyle\sum_{p=1}^{P} d_p\,(h) x_p^b(h) \\ -\gamma_h(\boldsymbol{x}^b, \Gamma_0) \geq 0, h \in \mathcal{H} \end{aligned} \quad (101)$$

$$\begin{aligned} x^a(h) - x^{g\delta}(h) + \underline{g}(h)\delta^g(h) + \textstyle\sum_{p=1}^{P} d_p\,(h) x_p^b(h) \\ -\gamma_h(\boldsymbol{x}^b, \Gamma_0) \geq \underline{g}(h), h \in \mathcal{H} \end{aligned} \quad (102)$$

$$\begin{aligned} x^a(h) - x^{g\delta}(h) + \overline{g}(h)\delta^g(h) + \textstyle\sum_{p=1}^{P} d_p\,(h) x_p^b(h) \\ +\gamma_h(\boldsymbol{x}^b, \Gamma_0) \leq \overline{g}(h), h \in \mathcal{H} \end{aligned} \quad (103)$$

where the protection function of the objective $\beta(\boldsymbol{x}^a, \Gamma_0)$ is defined in (70) and the protection functions of the inequality constraints $\gamma_h(\boldsymbol{x}^b, \Gamma_0)$ is defined as $\gamma_h(\Gamma_0)$ $(h \in \mathcal{H})$ in (71) (here (88) is used for the sake of notation simplicity).

Finally, removing unnecessary variables α and $\boldsymbol{x}^b$, it is straightforward transforming (96)-(103) into (63)-(69).

We finally remark that, in this formulation, the approach proposed in [35] is slightly modified. First, in [35] the uncertainty is modeled constrain-wise (i.e., perturbations of uncertain parameters in different constraints are not linked to each other). This allows defining for each constraint an individual budget of uncertainty, which represents the deviation allowed to the uncertain parameters affecting the given constraint. Conversely, in (96)-(103) only one Γ_0 is introduced to denote the total budget of uncertainty for all the parameters. In effect, the PH uncertain parameters $d_p(h)$ $(h \in \mathcal{H}, p \in \mathcal{P})$ simultaneously affect all the constraints (89)-(95). Second, in [35] there are as many separated protection functions as the unlinked constraints. On the other hand, in the above-defined approach, the definition of protection function in (70)-(73) is coupled to ensure the maximum variation for the entire set of uncertainty sources over the whole time horizon.

APPENDIX B

In this appendix, we provide the mathematical steps employed in transforming the robust counterpart from the min-max formulation (63)-(69) to the MIQP form (74)-(84).

We preliminarily note that (70)-(73) define a multi-objective optimization problem that aims at determining the portions $\Gamma_1, \dots, \Gamma_h, \dots, \Gamma_H$ of the uncertainty budget Γ_0 over all the time slots, which simultaneously maximize the values of the protection functions in the objective and constraints affected by uncertainty. This is formally expressed in the following lemma.

Lemma 1 (Protection functions as a solution of a multi-objective linear programming problem) - Protection functions $\beta(\boldsymbol{x}^a, \Gamma_0)$ and $\gamma_h(\Gamma_0)$ $(h \in \mathcal{H})$ defined in (70)-(73) equal to the optimal values of the objective functions in the following optimization problem:

$$\max_{\substack{\boldsymbol{u}_1,\dots,\\ \boldsymbol{u}_H,\Gamma_1,\\ \dots,\Gamma_H}} \begin{bmatrix} \sum_{h\in\mathcal{H}} 2k^+(h)|x^a(h)| \sum_{p\in\mathcal{P}} u_p(h)\hat{d}_p(h) \\ \sum_{p\in\mathcal{P}} u_p(1)\, \hat{d}_p(1) \\ \vdots \\ \sum_{p\in\mathcal{P}} u_p(H)\, \hat{d}_p(H) \end{bmatrix} \quad (104)$$

$$\text{s.t. } 0 \leq u_p(h) \leq 1, p \in \mathcal{P}, h \in \mathcal{H} \quad (105)$$

$$\sum_{p\in\mathcal{P}} u_p(h) \leq \Gamma_h, h \in \mathcal{H} \quad (106)$$

$$0 \leq \Gamma_h \leq P, h \in \mathcal{H}, \sum_{h\in\mathcal{H}} \Gamma_h = \Gamma_0. \quad (107)$$

Proof: The optimal solution of (104)-(107) consists in the optimal allocation $\Gamma_1^*, \dots, \Gamma_H^*$ (whose values are not necessarily integer) of the uncertainty budget Γ_0 among all the H slots in the time window $\mathcal{H}$ and, for each time slot $h \in \mathcal{H}$, the optimal assignment of supporting variables $u_1^*(h), \dots, u_P^*(h)$ representing the levels of variation related to all the P uncertainty sources in $\mathcal{P}$. For each $h \in \mathcal{H}$, $\lfloor \Gamma_h^* \rfloor$ of these variables are equal to 1, one of these is equal to $\Gamma_h^* - \lfloor \Gamma_h^* \rfloor$, and the remaining ones are equal to zero. This is equivalent to the selection of subsets $\{\mathcal{Q}_h \cup \{q_h\} | \mathcal{Q}_h \subseteq \mathcal{P}, |\mathcal{Q}_h| = \lfloor \Gamma_h \rfloor, q_h \in \mathcal{P} \setminus \mathcal{Q}_h\}$ $(h \in \mathcal{H})$ with corresponding cost functions in the arguments of (70) and additional constraints $\sum_{h\in\mathcal{H}} \Gamma_h = \Gamma_0$ and $0 \leq \Gamma_h \leq P, h \in \mathcal{H}$. □

We finally state the cornerstone of our investigation.

Theorem 1 (Robust counterpart as a MIQP problem) – Robust counterpart (63)-(69) has the equivalent MIQP formulation (74)-(84).

Proof: Preliminarily, we consider the dual of (104)-(107) based on the duality theory for multi-objective optimization [55]:

$$\min_{\substack{\Lambda\in\mathbb{R},\boldsymbol{\lambda}\in\mathbb{R}^H,\\ \Theta_{11},\dots,\Theta_{1H},\dots,\\ \Theta_{P1},\dots,\Theta_{PH}\in\mathbb{R},\\ \boldsymbol{\theta}_{11},\dots,\boldsymbol{\theta}_{1H},\dots,\\ \boldsymbol{\theta}_{P1},\dots,\boldsymbol{\theta}_{PH}\in\mathbb{R}^H}} \begin{bmatrix} \Gamma_0\Lambda + \sum_{p\in\mathcal{P}} \sum_{h\in\mathcal{H}} \Theta_{ph} \\ \Gamma_0\lambda(1) + \sum_{p\in\mathcal{P}} \sum_{h\in\mathcal{H}} \theta_{ph}(1) \\ \vdots \\ \Gamma_0\lambda(H) + \sum_{p\in\mathcal{P}} \sum_{h\in\mathcal{H}} \theta_{ph}(H) \end{bmatrix} \quad (108)$$

$$\text{s.t. } w_0\Lambda + \boldsymbol{w}^T\boldsymbol{\lambda} \geq 0 \quad (109)$$

$$w_0\Theta_{ph} + \boldsymbol{w}^T\boldsymbol{\theta}_{ph} \geq 0, p \in \mathcal{P}, h \in \mathcal{H} \quad (110)$$

$$\begin{aligned} w_0\left(\Lambda + \Theta_{ph} - 2k^+(h)\hat{d}_p(h)|x^a(h)|\right) \\ +\boldsymbol{w}^T\left(\boldsymbol{\lambda} + \boldsymbol{\theta}_{ph} - \hat{\boldsymbol{d}}_p\right) \geq 0, p \in \mathcal{P}, h \in \mathcal{H}. \end{aligned} \quad (111)$$

where the previously defined parameters $w_0, w_1, \dots, w_H$ correspond to the $(H+1)$ weights associated to the components in the mapping argument of (104). Note that in (108)-(111) we denote the $(H+1)$ dual variables of (106)-(107) (which can be compactly written as $\sum_{h\in\mathcal{H}} \sum_{p\in\mathcal{P}} u_p(h) \leq \Gamma_0$) as $\Lambda \in \mathbb{R}, \boldsymbol{\lambda} \in \mathbb{R}^H$ and the $(H+1)HP$ dual variables of (105) as $\Theta_{11}, \dots, \Theta_{PH} \in \mathbb{R}, \boldsymbol{\theta}_{11}, \dots, \boldsymbol{\theta}_{PH} \in \mathbb{R}^H$.

By theorem of strong duality for multi-objective optimization [55], optimal values of objective functions in

(108)-(111) and (104)-(107) coincide. Using Lemma 1, the protection functions $\beta(\boldsymbol{x}^a, \Gamma_0)$ and $\gamma_h(\Gamma_0)$ $(h \in \mathcal{H})$ equal to the optimal values of the objective functions in (108)-(111).

Let us define a new supporting variables vector $\boldsymbol{y} \triangleq |\boldsymbol{x}^a|$ by introducing the inequality constraints defined in (84). Consequently, (111) can be rewritten as:

$$\begin{aligned} & w_0\left(\Lambda + \Theta_{ph} - \tfrac{1}{2}k^+(h)\hat{d}_p(h)y(h)\right) \\ & +\boldsymbol{w}^T\left(\boldsymbol{\lambda} + \boldsymbol{\theta}_{ph} - \hat{\boldsymbol{d}}_p\right) \geq 0, p \in \mathcal{P}, h \in \mathcal{H}. \end{aligned} \tag{112}$$

Finally, replacing (108)-(110) and (112) into (63)-(69), we obtain that (63)-(69) is equivalent to MIQP problem (74)-(84).□

REFERENCES

[1] Y. Tan, Y. Cao, Y. Li, K. Y. Lee, L. Jiang and S. Li, "Optimal Day-Ahead Operation Considering Power Quality for Active Distribution Networks," *IEEE Trans. Autom. Sci. Eng.*, vol. 14, no. 2, pp. 425-436, April 2017.

[2] G. Brusco, A. Burgio, D. Menniti, A. Pinnarelli, N. Sorrentino, "Energy management system for an energy district with demand response availability," *IEEE Trans. Smart Grid*, 5(5), 2385–2393, Sep. 2014.

[3] Y. Fujimoto et al., "Distributed energy management for comprehensive utilization of residential photovoltaic outputs," *IEEE Trans. Smart Grid*, vol. 9, no. 2, pp. 1216-1227, Mar. 2018.

[4] M. Yousefi, A. Hajizadeh and M. Soltani, "Energy management strategies for smart home regarding uncertainties: State of the art, trends, and challenges," in *Proc. IEEE Int. Conf. Ind. Technol.*, 2018, 1219-1225.

[5] M. Rahmani-Andebili and H. Shen, "Energy scheduling for a smart home applying stochastic model predictive control," in *Proc. Int. Conf. Comput. Commun. Netw.*, Waikoloa, USA, 2016, 1-6.

[6] Y. Yang, Q. Jia, X. Guan, X. Zhang, Z. Qiu and G. Deconinck, "Decentralized EV-Based Charging Optimization With Building Integrated Wind Energy," *IEEE Trans. Autom. Sci. Eng.*, vol. 16, no. 3, pp. 1002-1017, 2019.

[7] Teng, F., & Strbac, G. (2017). Full stochastic scheduling for low-carbon electricity systems. *IEEE Trans. Autom. Sci. Eng.*, 14(2), 461-470.

[8] G.R. Aghajani, H.A. Shayanfar, H. Shayeghi, "Demand side management in a smart micro-grid in the presence of renewable generation and demand response," *Energy*, vol. 126, pp. 622-637, May 2017.

[9] Yan, B., Luh, P. B., Warner, G., & Zhang, P. (2017). Operation and design optimization of microgrids with renewables. *IEEE Trans. Autom. Sci. Eng.*, 14(2), 573-585.

[10] Verrilli, F., Srinivasan, S., Gambino, G., Canelli, M., Himanka, M., Del Vecchio, C., Sasso, M., & Glielmo, L. (2016). Model predictive control-based optimal operations of district heating system with thermal energy storage and flexible loads. *IEEE Trans. Autom. Sci. Eng.*, *14*(2), 547-557.

[11] A. Ouammi, Y. Achour, D. Zejli and H. Dagdougui, "Supervisory Model Predictive Control for Optimal Energy Management of Networked Smart Greenhouses Integrated Microgrid," *IEEE Trans. Autom. Sci. Eng.*, 2019. doi: 10.1109/TASE.2019.2910756.

[12] R. Carli and M. Dotoli, "Energy scheduling of a smart home under nonlinear pricing," in *Proc. IEEE Conf. Decis. Cont.*, Los Angeles, USA, 2014, pp. 5648-5653.

[13] R. Carli and M. Dotoli, "Decentralized control for residential energy management of a smart users' microgrid with renewable energy exchange," *IEEE/CAA J. Autom. Sin.*, 6(3), 641-656, 2019.

[14] C. Wang et al., "Robust-index method for household load scheduling considering uncertainties of customer behavior,'' *IEEE Trans. Smart Grid.*, vol. 6, no. 4, pp. 1806–1818, Mar. 2015.

[15] B. Kim, Y. Zhang, M. van der Schaar, J. Lee, "Dynamic pricing and energy consumption scheduling with reinforcement learning," *IEEE Trans. Smart Grid*, vol. 7, no. 5, pp. 2187-2198, 2016.

[16] A. Mohsenian-Rad, V.W.S. Wong, J. Jatskevich, R. Schober, "Optimal and autonomous incentive-based energy consumption scheduling algorithm for smart grid," in *Proc. Innov. Smart Grid Technol.*, Gothenburg, Sweden, 2010, pp. 1-6.

[17] J. Yue, Z. Hu, A. Anvari-Moghaddam, J.M. Guerrero, "A multi-market-driven approach to energy scheduling of smart microgrids in distribution networks," *Sustainability*, vol. 11, no. 2, pp. 1-16, Jan. 2019.

[18] B. Rajasekhar, N. Pindoriya, W. Tushar and C. Yuen, "Collaborative energy management for a residential community: a non-cooperative and evolutionary approach," *IEEE Trans. Emerg. Top. Comput. Intell.*, vol. 3, no. 3, pp. 177-192, June 2019.

[19] P. Samadi, R. Schober, V.W.S. Wong, "Optimal energy consumption scheduling using mechanism design for the future smart grid," in *proc. IEEE Smart Grid Commun*., Brussels, Belgium, 2011, pp. 369-374.

[20] M.H.K. Tushar, C. Assi, M. Maier, M.F. Uddin, "Smart microgrids: optimal joint scheduling for electric vehicles and home appliances," *IEEE Trans. Smart Grid*, vol. 5, no. 1, pp. 239–250, Jan. 2014.

[21] J. Yue, Z. Hu, C. Li, J.C. Vasquez, J.M. Guerrero, "Economic power schedule and transactive energy through an intelligent centralized energy management system for a DC residential distribution system," *Energies*, vol. 10, no.7, pp. 1-14, July 2017.

[22] T. T. Kim and H. V. Poor, "Scheduling power consumption with price uncertainty," *IEEE Trans. Smart Grid*, vol. 2, no. 3, pp. 519-527, Sept. 2011.

[23] X. Wu, X. Hu, X. Yin, and S. Moura, "Stochastic optimal energy management of smart home with PEV energy storage," *IEEE Trans. Smart Grid*, vol. 9, no. 3, pp. 2065-2075, May 2018.

[24] J. Munkhammara, J. Widén and J. Rydén "On a probability distribution model combining household power consumption, electric vehicle home-charging and photovoltaic power production," *Applied Energy*, vol. 142, pp. 135-143, Mar. 2015.

[25] F. Teng and G. Strbac, "Full stochastic scheduling for low-carbon electricity systems," *IEEE Trans. Autom. Sci. Eng.*, vol. 14, no. 2, pp. 461-470, Apr. 2017.

[26] P. Kou, D. Liang and L. Gao, "Stochastic energy scheduling in microgrids considering the uncertainties in both supply and demand," *IEEE System. Journal.*, vol. 12, no. 3, pp. 2589-2600, Sept. 2018.

[27] Z. Chen, L. Wu, Y. Fu, "Real-time price-based demand response management for residential appliances via stochastic optimization and robust optimization," *IEEE Trans. Smart Grid*, vol. 3, no. 4, pp. 1822-1831, Dec. 2012.

[28] L. Guo, H. Wu, H. Zhang, T. Xia and S. Mehraeen, "Robust optimization for home-load scheduling under price uncertainty in smart grids," in *Proc. IEEE Int. Conf. Comp. Comm*, Garden Grove, USA, 2015, 487–493.

[29] C. Zhang, Y. Xu, Z. Y. Dong and J. Ma, "Robust operation of microgrids via two-stage coordinated energy storage and direct load control," *IEEE Trans. Power Syst.*, vol. 32, no. 4, pp. 2858-2868, July 2017.

[30] W. Yi, Y. Zhang, Z. Zhao, Y. Huang, "Multiobjective robust scheduling for smart distribution grids: considering renewable energy and demand response uncertainty," *IEEE Access*, vol. 6, pp. 45715-45724, Aug. 2018.

[31] C. Wang, Y. Zhou, B. Jiao, D. Wang, "Robust optimization for load scheduling of a smart home with photovoltaic system," *Energ. Convers. Manag.*, vol. 102, pp. 247-257, Sept. 2015.

[32] S. Paul and N. P. Padhy, "Resilient scheduling portfolio of residential devices and plug-in electric vehicle by minimizing conditional value at risk," *IEEE Trans. Industr. Inform.*, vol. 15, no. 3, pp. 1566-1578, Mar. 2019.

[33] A. Hussain, V. Bui and H. Kim, "Robust optimal operation of ac/dc hybrid microgrids under market price uncertainties," *IEEE Access*, vol. 6, pp. 2654-2667, Aug. 2018.

[34] K. Paridari, A. Parisio, H. Sandberg, K.H. Johansson, "Robust scheduling of smart appliances in active apartments with user behavior uncertainty," *IEEE Trans. Autom. Sci. Eng.*, vol. 13, no. 1, pp. 247-259, Jan. 2016.

[35] H.H. Doulabi, P. Jaillet, G. Pesant, L.M. Rousseau, "Exploiting the structure of two-stage robust optimization models with exponential scenarios," *INFORMS Journal on Computing*, 2019.

[36] B. Zeng, L. Zhao, "Solving two-stage robust optimization problems using a column-and-constraint generation method," *Operations Research Letters*, vol. 41, no. 5, pp. 457-461, Sept. 2013.

[37] A. Ben-Tal, A. Goryashko, E. Guslitzer, A. Nemirovski, "Adjustable robust solutions of uncertain linear programs," *Math Program*, vol. 99, no. 2, pp. 351-376, 2004.

[38] A. Ben-Tal, G. Boaz, S. Shimrit, "Robust multi-echelon multi-period inventory control," *European Journal of Operational Research*, vol. 199, no. 3, pp. 922-935, 2009.

[39] A. Ouorou, G. Boaz, S. Shimrit, "Tractable approximations to a robust capacity assignment model in telecommunications under demand uncertainty," *Computers & Operations Research*, 40(1), 318-327, 2013.

[40] D. Bertsimas, D.B. Brown, C. Caramanis, "Theory and applications of robust optimization," *SIAM Rev*, vol. 53, no. 3, pp. 464-501, 2011.

[41] F.J.C.T. de Ruiter, A. Ben-Tal, R.C.M. Brekelmans, D.D. Hertog " Robust optimization of uncertain multistage inventory systems with inexact data in decision rules," *Comput Manag Sci*, vol. 14, pp. 45-66, 2017.

[42] D. Bertsimas and M. Sim, "The price of robustness," *Oper. Res.*, vol. 52,

no.1, pp. 35-53, Feb. 2004.
[43] X. Wu, Z. Wang, J. Du and G. Wu, "Optimal Operation of Residential Microgrids in the Harbin Area," *IEEE Access*, 6, 30726-30736, 2018.
[44] M. Ahmadi, J. M. Rosenberger, W. Lee and A. Kulvanitchaiyanunt, Optimizing Load Control in a Collaborative Residential Microgrid Environment, *IEEE Trans. Smart Grid*, 6(3), 1196-1207, 2015.
[45] X. Yang, Y. Zhang, H. Wu and H. He, "An Event-Driven ADR Approach for Residential Energy Resources in Microgrids With Uncertainties," *IEEE Trans. Ind. Electron.*, 66(7), 5275-5288, 2019.
[46] A. Anvari-Moghaddam, J. M. Guerrero, J. C. Vasquez, H. Monsef and A. Rahimi-Kian, "Efficient energy management for a grid-tied residential microgrid," *IET Generation, Transmission & Distribution*, vol. 11, no. 11, pp. 2752-2761, August 2017.
[47] K. D. Orwig *et al.*, "Recent Trends in Variable Generation Forecasting and Its Value to the Power System," in *IEEE Trans. Sustain. Energy*, vol. 6, no. 3, pp. 924-933, July 2015.
[48] Kong, W., Dong, Z. Y., Hill, D. J., Luo, F., & Xu, Y. "Short-term residential load forecasting based on resident behaviour learning". *IEEE Trans. Power Syst.*, *33*(1), 1087-1088, 2017.
[49] Esther, B. P., & Kumar, K. S. "A survey on residential demand side management architecture, approaches, optimization models and methods". *Renewable and Sustainable Energy Reviews*, 59, 342-351, 2016.
[50] Ramanathan, B., Vittal, V. "A framework for evaluation of advanced direct load control with minimum disruption". *IEEE Trans. Power Syst.*, 23(4), 1681-1688, 2008.
[51] V. Monteiro, H. Gonçalves, J.C. Ferreira, J. L. Afonso, J. P. Carmo and J. E. Ribeiro, "Batteries charging systems for electric and plug-in hybrid electric vehicles," In *New Advances in Vehicular Technology and Automotive Engineering*, InTech, pp. 149-168, 2012.
[52] A. Parisio, E. Rikos, and L. Glielmo, "A model predictive control approach to microgrid operation optimization," *IEEE Trans. Control Syst. Technol.*, vol. 22, no. 5, pp.1813–1827, 2014.
[53] Z. Liu, C. Zhang, M. Dong, B. Gu, Y. Ji and Y. Tanaka, "Markov-decision-process-assisted consumer scheduling in a networked smart grid," in *IEEE Access*, vol. 5, pp. 2448-2458, 2017.
[54] A. Bemporad and M. Morari, "Control of systems integrating logic, dynamics, and constraints," *Automatica*, vol. 35, no. 3, pp. 407–427, 1999.
[55] G. Wanka and R. I. Boţ, "Multiobjective duality for convex-linear problems II,". *Mathematical Methods of Operations Research*, vol. 53, no. 3, pp. 419-433, 2001.
[56] S. Rezzonico, S. Nowak, "Buy-back rates for grid-connected photovoltaic power systems," *IEA PVPS Task 1, Report IEA PVPS TI*, Nov. 1997.
[57] Eurostat, Electricity prices for household consumers - bi-annual data (from 2007 onwards), *available at*: http://appsso.eurostat.ec.europa.eu/nui/show.do?dataset=nrg_pc_204&lang=en (accessed on 30 April 2019).
[58] A. Alberini, G. Prettico, C. Shen, J. Torriti,"Hot weather and hourly electricity demand in Italy," *Energy*, vol. 177, pp. 44-56, June 2019.
[59] N. Tutkun, Ö. Can and E. S. Şan, "Daily cost minimization for an off-grid renewable microhybrid system installed to a residential home," in *proc. International Conference on Renewable Energy Research and Applications*, Palermo, Italy, pp. 750-754, 2015.
[60] Soyster, A. L. "Convex programming with set-inclusive constraints and applications to inexact linear programming". *Oper. Res.* 21 1154–1157, 1973.
[61] Hubert T., Grijalva S. "Modeling for residential electricity optimization in dynamic pricing environments". *IEEE Trans Smart Grid*; 3(4):2224–31, 2012.

Seyed Mohsen Hosseini (S'19) received the B.S. degree from the Shahed University, Tehran, Iran, in 2010, and the M.S. degree from the Semnan University, Semnan, Iran, in 2013, both in Electrical Engineering.

He is currently working toward the Ph.D. degree in the Department of Electrical and Information Engineering, Politecnico di Bari, Bari, Italy. His research interests include modeling, optimization and control of energy systems, distributed control systems, robust control and model predictive control.

Raffaele Carli (M'17) received the Laurea degree in electronic engineering with honours in 2002 and the Ph.D. in Electrical and Information Engineering in 2016, both from Politecnico di Bari, Italy. From 2003 to 2004, he was a Reserve Officer with Italian Navy. From 2004 to 2012, he worked as System and Control Engineer and Technical Manager for a space and defense multinational company.

Dr. Carli is now a research fellow at Politecnico di Bari, and his research interests include the formalization, simulation, and implementation of decision and control systems, as well as modeling and optimization of complex systems.

Mariagrazia Dotoli (M'96, SM'12) received the Laurea degree in electronic engineering with honours in 1995 and the Ph.D. in electrical engineering in 1999 from Politecnico di Bari (Italy).

She has been a visiting scholar at the Paris 6 University and at the Technical University of Denmark. She is expert evaluator of the European Commission since the 6th Framework Programme. She is a Full Professor in Automatic Control at Politecnico di Bari, which she joined in 1999. She has been the Vice Rector for research of Politecnico di Bari and a member elect of the Academic Senate. Her research interests include modeling, identification, management, control and diagnosis of discrete event systems, manufacturing systems, logistics systems, traffic networks.

Prof. Dotoli was co-chairman of the Training and Education Committee of ERUDIT, the European Commission network of excellence for fuzzy logic and uncertainty modeling in information technology, and was key node representative of EUNITE, the EUropean Network of excellence on Intelligent Technologies. She is the Editor in Chief of the IEEE SYSTEMS MAN AND CYBERNETICS SOCIETY E-NEWSLETTER, and an Associate Editor of the IEEE TRANS. ON AUTOMATION SCIENCE AND ENGINEERING, and of the IEEE TRANS. ON CONTROL SYSTEMS TECHNOLOGY. She is the Program chair of the 2020 IEEE Conference on Automation Science and Engineering. She was the Program co-chair of the 2017 IEEE Conference on Automation Science and Engineering, the Workshop and Tutorial chair of the 2015 IEEE Conference on Automation Science and Engineering, the Special Session co-chair of the 2013 IEEE Conference on Emerging Technology and Factory Automation and chair of the National Committee of the 2009 IFAC Workshop on Dependable Control of Discrete Systems. She was member of the International Program Committee of 70+ international conferences. She is author of 200+ publications, including 1 textbook (in Italian) and 60+ international journal papers.